

©[May, 2012]

PING WANG

ALL RIGHTS RESERVED

**Molecular Mobility of Amorphous Disaccharides Films by Phosphorescence of
Various Probes with Indole Chromophore Group**

By

PING WANG

A thesis submitted to the

Graduate School-New Brunswick

Rutgers, The State University of New Jersey

in partial fulfillment of the requirements

for the degree of

Master of Science

Graduate Program in Food Science

Written under the direction of

Dr. Richard D. Ludescher

And approved by

New Brunswick, New Jersey

[May, 2012]

ABSTRACT OF THE THESIS

Molecular Mobility of Amorphous Disaccharides Films by Phosphorescence of Various Probes with Indole Chromophore Group

By PING WANG

Thesis Director: Dr. Richard D. Ludescher

Amorphous solids lack the long-range order of crystalline solids. Their molecular mobility properties not only modulate the biological properties of seeds, spores and some organisms during anhydrobiosis, but also control the stability and quality of pharmaceuticals, dried and frozen foods.

Tryptophan phosphorescence in proteins provides a sensitive long-lived signal of molecular mobility of the local environment in amorphous sugar matrix. However, there are many factors that need to be studied for a better understanding of the relationship between tryptophan triplet-state lifetimes in proteins and molecular mobility of the local environment. Those factors include the molecular structure of probes and matrix, intermolecular and intramolecular reaction, water content in the matrix, temperature and so on.

The object of this research is to investigate how different groups on

phosphorescent probes as well as two different disaccharide matrix influence on non-radiative phosphorescence decay rate at a wide temperature range, and to discuss the possible inter- or/and intra- molecular interaction among probes, water, and disaccharide molecules. Sucrose and trehalose are utilized here as amorphous disaccharide to evaluate how the probes differ in their response to matrix dynamics. And we here used 14 different probes including indole, tryptophan, tryptophanamide, N-acetyltryptophan, N-acetyltryptophanamide, 5-hydroxytryptophan, 5-methyltryptophan, 4-fluorotryptophan, 6-fluorotryptophan, 5-bromotryptophan, the dipeptides Trp-Gly and Gly-Trp, and 20-residue Trp-cage protein.

Measurements of phosphorescence lifetime for all those triplet state probes in amorphous sucrose and trehalose films as a function of temperature provide data implying significant mobility in the amorphous sugars in the glassy state as well as at the glass-to-melt transition. Generally, all those probes except 5-Br-Trp have an extreme sensitivity of the triplet excited state decay processes to the local environment. Since amorphous trehalose have more packed structure with higher T_g than amorphous sucrose, the molecular mobility in trehalose film are less influenced by temperature and more restricted than one in sucrose over the temperature range from -10 °C to 120 °C, which is observed by using all different probes in these two films. In all, most probes provide similar trends of the mobility in amorphous sugar film over a wide temperature range, while there are subtle differences among probes.

ACKNOWLEDGEMENT

I would like to thank my advisor Dr. Richard Ludescher for all his encouragement and advising. Also, I would like to thank my lab mates Andrew, Jun, Maria, Melinda, Sanaza for great environment in the lab. At last, a special thanks to my best friends and my loving family. With your support and understanding, the process was much easier and enjoyable.

LIST OF TABLES

Table 1: Chemical Structure and glass transition temperatures of sucrose and trehalose.....	14
---	----

LIST OF FIGURES

Figure 1: Jablonski energy diagram.....	8
Figure 2: Structures of the phosphorescence small molecule probes used in this study	16
Figure 3: Structure of 20-residue Trp-cage protein	17
Figure 4: Normalized fluorescence emission and excitation spectra of some probes	24
Figure 5: Normalized phosphorescence emission and excitation spectra of some probes	25
Figure 6: Normalized intensity (a.u.) vs. time for various probes in amorphous trehalose, including indole, tryptophan, 5-Br-Trp, 5-OH-Trp, NATA, and Gly-Trp	31
Figure 7: Normalized intensity in logarithmic scale vs. time for various probes in amorphous trehalose, including indole, tryptophan, 5-Br-Trp, 5-OH-Trp, NATA, and Gly-Trp.....	32
Figure 8: Phosphorescence intensity decays of Trp-cage in amorphous trehalose film at -10 °C	33
Figure 9: Modified residuals ((data-fit)/data ^{1/2}) vs. time for Trp-cage protein in amorphous trehalose film at -10 °C	34
Figure 10: Average lifetime (τ_i) vs. temperature of Trp-cage protein in amorphous trehalose film	35

Figure 11: Average amplitude (a_i) vs. temperature of Trp-cage protein in amorphous trehalose film	36
Figure 12: Average amplitude (a_i) at corresponding decay time (τ_i) of Trp-cage protein in amorphous trehalose film	37
Figure 13: $\ln(k_{NR})$ as a function of temperature for Trp-cage protein in amorphous trehalose film	38
Figure 14: The activation energy as a function of temperature for Trp-cage protein in amorphous trehalose film	39
Figure 15: $\log(k_{NR}/s-1)$ vs. K/T in amorphous trehalose film for 12 probes including indole, Trp, TA, NAT, NATA, 5-methyl-Trp, 5-OH-Trp, 7-Aza-Trp, Trp-Gly, Gly-Trp, Trp-cage protein, and HSA	40
Figure 16: $\log(k_{NR}/s-1)$ vs. K/T in amorphous sucrose film for 12 probes including indole, Trp, TA, NAT, NATA, 5-methyl-Trp, 5-OH-Trp, 7-Aza-Trp, Trp-Gly, Gly-Trp, Trp-cage protein, and HSA	41
Figure 17: Activation energy vs. $T/^{\circ}C$ in amorphous trehalose film for 7 probes including indole, Trp, 5-OH-Trp, NATA, Gly-Trp, Trp-cage protein, and HSA.....	42
Figure 18: Activation energy vs. $T/^{\circ}C$ in amorphous sucrose film for 7 probes including indole, Trp, 5-OH-Trp, NATA, Gly-Trp, Trp-cage protein, and HSA	43
Figure 19: Comparison of Arrhenius analysis of non-radiative phosphorescence decay rate as a function of temperature for selected probes in amorphous	

sucrose and trehalose matrix.....	48
Figure 20: Comparison of $\log(s/\tau)$ vs. K/T for selected probes in amorphous sucrose and trehalose	49
Figure 21: Comparison of Arrhenius analysis of non-radiative phosphorescence decay rate as a function of temperature for indole and tryptophan in amorphous sucrose and trehalose matrix	52
Figure 22: Comparison of Arrhenius analysis of non-radiative phosphorescence decay rate as a function of temperature for tryptophan, Trp-Gly, and Gly-Trp in amorphous sucrose and trehalose matrix	54
Figure 23: Comparison of the most stable conformer of Trp-Gly and Gly-Trp	55
Figure 24: The most stable conformer of Trp-Gly	55
Figure 25: Comparison of Arrhenius analysis of non-radiative phosphorescence decay rate as a function of temperature for NAT, TA, Trp-Gly, and Gly-Trp in amorphous sucrose and trehalose matrix	57
Figure 26: Arrhenius analysis of non-radiative phosphorescence decay rate as a function of temperature for TA, NAT, NATA, and tryptophan in sucrose and trehalose matrix.	59
Figure 27: Arrhenius analysis of non-radiative phosphorescence decay rate as a function of temperature for tryptophan, 5-hydroxyl-tryptophan, 5-methyl-tryptophan in sucrose and trehalose matrix	61
Figure 28: Arrhenius analysis of phosphorescence lifetime as a function of temperature for tryptophan, 5-bromotryptophan, 4-fluorotryptophan and	

6-fluorotryptophan in amorphous sucrose and trehalose matrix	64
Figure 29: Arrhenius analysis of non-radiative phosphorescence decay rate as a function of temperature for tryptophan and 7-azatryptophan in sucrose and trehalose matrix	67
Figure 30: Arrhenius analysis of non-radiative phosphorescence decay rate as a function of temperature for tryptophan, 20-residue Trp-Cage protein, and human serum albumin(HSA) in sucrose and trehalose matrix	70
Figure 31: Lowest level energy structure of Trp-Cage protein	71

TABLE OF CONTENTS

ABSTRACT OF THE THESIS	ii
ACKNOWLEDGEMENT.....	iv
LIST OF TABLES	v
LIST OF FIGURES	vi
LIST OF CONTENT	x
INTRODUCTION	1
AMORPHOUS SOLIDS	2
PHOTOPHYSICS OF LUMINESCENCE.....	5
PHOSPHORESCENCE OF AMORPHOUS SUGAR FILMS WITH VARIOUS PROBES.....	9
MATERIALS AND METHODS	15
CHEMICALS	15
SAMPLE PREPARATION	18
LUMINESCENCE MEASUREMENT	18
RESULTS AND DISCUSSION	22
1. EXCITATION AND EMISSION SPECTRA OF LUMINESCENCE FOR PROBES IN AMORPHOUS SUGAR MATRIX.	22
1.1 Luminescence Excitation Spectra.....	22
1.2 Luminescence Emission Spectra	22

2. PHOSPHORESCENCE INTENSITY DECAY	26
3. VARIATION OF PHOSPHORESCENCE NON-RADIATIVE DECAY RATE (K_{NR}) AND ACTIVATION ENERGY (EA) IN AMORPHOUS SUCROSE AND TREHALOSE	44
4. COMPARISON OF INDOLE, TRP, TA, NAT, NATA, TRP-GLY AND GLY-TRP	50
4.1. Indole and Trp.....	50
4.2. Trp, Gly-Trp and Trp-Gly	53
4.3. Gly-Trp vs. NAT and Trp-Gly vs. TA	57
4.4. Trp, TA, NAT and NATA.....	59
5. COMPARISON OF TRYPTOPHAN, 5-HYDOXYLTRYPTOPHAN AND 5-METHYLTRYPTOPHAN	61
6. COMPARISON OF TRYPTOPHAN AND 4-FLUOROTRYPTOPHAN, 6-FLUOROTRYPTOPHAN, AND 5-BROMOTRYPTOPHAN	63
7. COMPARISON OF TRYPTOPHAN AND 7-AZATRYPTOPHAN	66
8. COMPARISON OF TRYPTOPHAN, TRP-CAGE PROTEIN AND HSA	70
CONCLUSION.....	75
REFERENCES	78

INTRODUCTION

Phosphorescence spectroscopy is a very sensitive, site-specific technique to detect molecular mobility of triplet state probes within the local environment (Richert, 2000). In our lab, tryptophan phosphorescence has been applied to study the protein dynamic in the amorphous sugar matrix, which can help to explain how the integration of protein into amorphous sugar molecules instead of water prolongs the stability of protein (Draganski and Ludescher, 2010). Tryptophan is one of the rarest amino acids, which compose about 1% of the residues in globular proteins, but phosphorescence of the rare tryptophan is sensitive enough to provide a site specific probe of protein structure, dynamics, and function (McCaul and Ludescher, 1999). But, a better understanding of the mechanisms governing the tryptophan triplet-state lifetimes is needed to have more accurate interpretation of phosphorescence studies of proteins (Fisher et al., 2001; Gonnelli and Strambini, 2005). First, single protein is a macromolecule with complex structure, so there are many possible interactions of the excited state by protein itself and/or by protein and sugar, which may affect tryptophan photophysical behavior and measured parameters. For example, groups surrounded tryptophan residue may promote proton transfer, hydrogen bonding, formation of charge transfer complexes, and so on. In this case, quenching of tryptophan phosphorescence due to the effects of surrounding groups in protein can be incorrectly interpreted as quenching resulting from intermolecular interaction by protein and sugar. Moreover, tryptophan residue in nature protein is fixed so that the signal received from tryptophan phosphorescence may not enough to understand the

whole dynamic of the protein in amorphous sugar matrix. For example, the tryptophan residue in protein exposure to amorphous sugar matrix as well as the one buried in the protein can show different phosphorescence results corresponding to their local environment. At the same time, it is a problem to use tryptophan phosphorescence to test protein dynamic for some nature proteins which do not have any tryptophan residue. Therefore, in many study extrinsic probes are applied as well as mutated protein with tryptophan or tryptophan analogues at the specific sites. In all, since complexity of protein structure and limited application of tryptophan in nature protein, it is much clear for us by using small fluorescent probes to understand firstly how tryptophan phosphorescence would be influenced by specific surrounding groups in probes as well as sugar molecules. In this study, 14 different small molecules containing indole chromophore are utilized as phosphorescence probes to investigate the above mechanisms in amorphous sugar films.

Amorphous solids

There are two types of solids, crystalline solids and amorphous solids (glass). Both of them have the essential attributes of solid state, but their microscopic structures and dynamic properties are fundamentally different. The arrangement of atoms in amorphous solids lacks the long-range order of crystalline solids. However, the amorphous solids do not act like a gas with random distribution of molecules either. Molecules in amorphous solids have a high degree of local correlation with local energy minimum configurations. Moreover, only vibrational motion is available in

crystalline solids, while limited rotational and translational motion are also available in amorphous solids. Furthermore, in the plots of volume versus temperature it has been showed that the solidification from liquid to an amorphous solid is continuous with intermediate glass transition, while the solidification from liquid to a crystalline solid state is discontinuous with no intermediate transition (Zallen, 1983). Crystalline solids have the melting transition from order to disorder at melting point, T_m , and amorphous solids have the softening transition from glass to rubber/melt at glass transition temperature, T_g .

Amorphous solids are not only technological applied as structural materials (organic glass), semiconductor and ultratransparent optical fiber, but also are broadly found in polymer, foods, pharmaceuticals materials and biological objectives. Their molecular mobility properties can modulate the biological properties of seeds, spores and some organisms during anhydrobiosis (Sun and Leopold, 1997), as well as control the stability and quality of pharmaceuticals (Hancock et al., 1995), and dried and frozen foods (Fennema, 1996). Amorphous solids in food products can be formed by destructive processing, like rapid cooling of liquid melt, spray drying, freeze drying, extrusion, grinding, milling and so on (Zallen, 1983; Liu et al., 2006). Amorphous state is important for many food products, e.g. frozen foods (ice cream), and dried foods (sugar candy and milk powder). The high viscosity of amorphous state can improve the stability of food system in order to prolong the storage time of those foods (Goff et al., 1993; Jouppila and Roos, 1994; Bhandari and Howes, 1998).

The amorphous state is considered to be a non-equilibrium state (Fennema, 1976). T_g , the glass transition temperature, is a kinetic parameter and is defined as the temperature range corresponding to the glass-liquid transition. It is recognized that T_g is an important index temperature for food stability. At low temperature (below T_g), amorphous solids in glass state are hard and rigid because the molecules can only undergo vibrational and limited rotational motions, while at high temperature (above T_g) amorphous solids go through glass-melt transition and become soft and flexible because of the onset of translational motion above T_g . For polymer materials, the supercooled melt at temperature between T_g and T_m (melting temperature) is named as rubber; For low molecular weight material, it is a mainly viscous liquid and is called as melt.

The mobility of amorphous solids is very important issue on the stability of many foods (frozen foods, dried and semidried foods), because it can modulate texture, and both rates of chemical reactions and physical changes, such as gelatinization of starch, structural collapse, solute diffusion, crystallization, and maillard reaction and so on (Fennema, 1976) . Currently, T_g , the onset temperature for cooperative translational motion in amorphous solids, is recognized as an important index for food stability. However, T_g is not enough to relate food stability with molecular mobility of amorphous solids. And a lot of research has showed that chemical stability may not be related to global mobility (Yoshioka and Aso, 2007; Rossi et al., 1997). The molecular vibrational and rotational motions below T_g , the translational mobility of water below

T_g , and the heterogeneity of amorphous matrix all can have a significant influence on food stability (Ludescher et al., 2001; Yoshioka and Aso, 2007). Since the complex of chemical compositions and its distribution, food materials are always complicated and have little known about glass and sub-glass relaxation compared to nonfood materials (Liu et al., 2006). In all, the further understanding of molecular mobility in amorphous food model is needed to improve the shelf-life and quality of the above foods.

Photophysics of Luminescence

Luminescence, including fluorescence and phosphorescence, is the emission of light from a substance and occurs from electronically excited states. Fluorescence occurs from an excited singlet state while phosphorescence occurs from an excited triplet state. The photophysical events of fluorescence and phosphorescence are showed by the Jablonski energy diagram (Fig. 1).

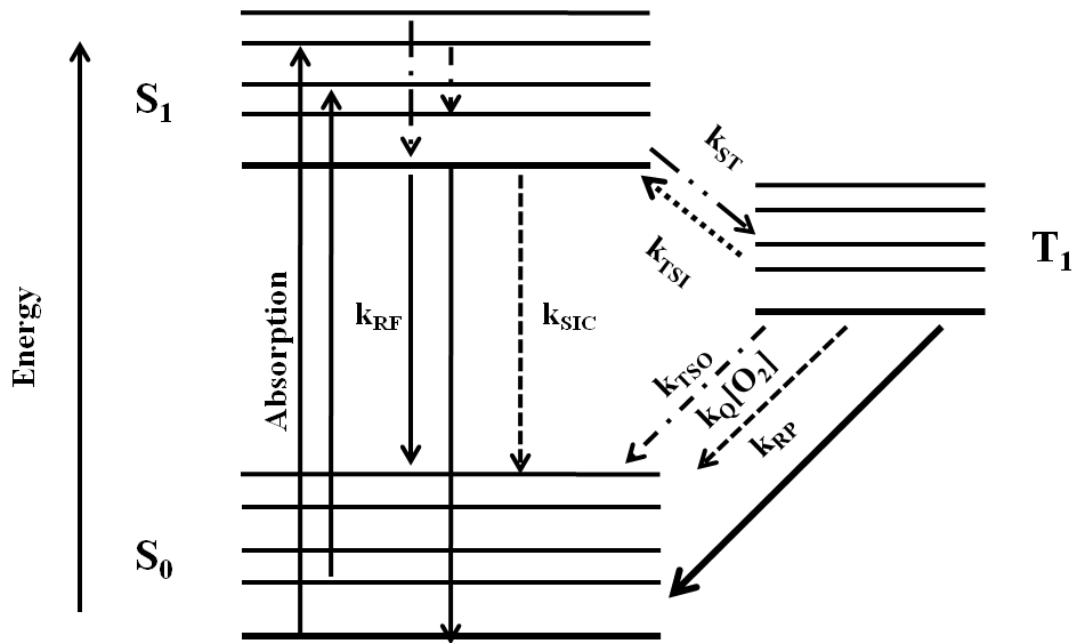
Before light absorption, molecules stay in the lowest energy level of the singlet ground state (S_0). In this state, all electron spins are paired (paired spins). Following light absorption, molecules have a higher energy level and make an essentially instantaneous transition (10^{-14} to 10^{-15} s) to one of the vibrational levels in the excited singlet state (S_1), while molecules with excess vibrational energy relax rapidly to the lowest vibrational level of S_1 . The electron spins in the excited singlet state are still paired. Then, molecules in the lowest vibrational level of S_1 can relax to the ground

state by fluorescence (a radiative process) or by internal conversion (a non-radiative process). At the same time, molecules in the lowest level of S_1 can be modified by intersystem crossing to the excited triplet state T_1 , which is less energetic than S_1 . Electron spins in the T_1 state are unpaired (parallel). Also, molecules in the T_1 state can have de-excitation process to go back to ground state by many ways: phosphorescence (a radiative process), non-radiative decay from T_1 to S_0 , and collisional quenching (especially oxygen quenching). One more possible process that should be mentioned here is molecules in the T_1 state can undergo reverse intersystem crossing from T_1 to S_1 , which gives rise to delayed fluorescence.

The rate constant of fluorescence (k_{RF}) and phosphorescence (k_{RP}) are fixed by the probe structure and not influenced by environment, like temperature or the matrix. However, the rate constants of internal conversion (k_{SIC}) from S_1 to S_0 , non-radiative decay (k_{TSO}) from T_1 to S_0 and quenching ($k_Q[Q]$) of excited triplet state are influenced by temperature as well as matrix. k_{NR} , which is used in the following chapter, stands for total phosphorescence non-radiative decay rate ($k_{NR} = k_{TSO} + k_Q[O_2]$). In our study, since we apply nitrogen to avoid oxygen quenching, the value of $k_Q[Q]$ of the excited triplet state is ignored and the value of k_{NR} is equal to the value of k_{TSO} here.

Since the spin state of electrons in the T_1 (unpaired) is different from the one in the S_1 and S_0 (paired), phosphorescence decay does involve a change in electron spin

direction while fluorescence decay does not. Therefore, emission from the excited triplet state is much slower than emission from the excited singlet state. Fluorescence is thus a much faster event than phosphorescence. Fluorescence occurs in 10^{-9} to 10^{-7} s, while phosphorescence occurs in 10^{-3} to 10^2 s. The experimentally accessible timescale for molecular mobility measurement is largely determined by the excited state emission lifetime. Normally, the emission lifetime should be longer than the timescale of detected molecular motion. Hence, fluorescence is usually applied to detect molecular motion on the nanosecond timescale while phosphorescence is utilized to monitor the motions on microsecond timescale and larger.



Jablonski Energy Diagram

Fig. 1. Jablonski energy diagram. S_0 : singlet ground state. S_1 : excited singlet state. T_1 : excited triplet state. k_{RF} : rate constant for fluorescence decay from S_1 to S_0 . k_{SIC} : rate constant for non-radiative decay rate from S_1 to S_0 . k_{ST} : rate constant for intersystem crossing from S_1 to T_1 . k_{TSI} : rate constant for reverse intersystem crossing from T_1 to S_1 . k_{TSO} : rate constant for non-radiative decay from T_1 to S_0 . $k_Q[O_2]$: rate constant for oxygen quenching of excited triplet state. k_{RP} : rate constant for radiative decay from T_1 to S_0 .

Phosphorescence of amorphous sugar films with various probes

Amorphous carbohydrates are very widely used in foods and pharmaceuticals and are important components of biological materials (Levine, 2002; Sun and Leopold, 1997). Water is a strong plasticizer of amorphous carbohydrates and has a strong influence on the glass transition temperature. Because the water has an enormous plasticizing effect on sugars, the T_g values must be reported together with moisture content in order to avoid confusion (Hancock and Dalton, 1999; Noel et al., 2000). In the Table 1, it shows the T_g of sucrose and trehalose when their water concentration is about 0 ~1 wt%.

Like other amorphous solids, glassy sugar shows dynamic heterogeneity. Probes mixed within the amorphous sugar have heterogeneous local environment, which may be caused by local difference in packing interaction among molecules in the amorphous sugar. Probes with more constrained interactions in the local environment (e.g. hydrogen bonding interaction) would show longer phosphorescence lifetime due to slower/fewer molecular collisions that quench the triplet state, since in this case the molecule mobility of local environment is generally lower. In contrast, if probes have less constrained interactions with surrounding sugar molecules, they would have shorter phosphorescence lifetime because of faster/more molecular collisions that quench the triplet state, and the molecule mobility of local environment is overall faster. Hence, probes in amorphous solids can have distinct regions and show different relaxation times.

Numerous experimental techniques are used to characterize molecular mobility of amorphous solids like NMR, dielectric spectroscopy, DSC, and luminescence spectroscopy (Noel et al., 2000; Zhou et al., 2002; Hancock et al., 1995) Ludescher and colleagues have already used phosphorescence spectroscopy to study dynamic site heterogeneity in various amorphous solids (Pravinata et al., 2005; Shirke et al., 2006).

Both prompt fluorescence and delayed phosphorescence can provide site-specific information about molecular mobility. This information includes not only direct information about the rotational motions of the luminescent chromophore, but also indirect information about the molecular mobility of the local environment surrounding the chromophore. Due to the slow molecular motion in amorphous solids, phosphorescence is more sensitive than fluorescence to deactivation by collisions with solvent molecules, quenchers and energy transfer processes.

Tryptophan is a naturally existing amino acid, which probably compose only about 1% of the residues in gluten proteins. Fluorescence and phosphorescence of tryptophan is sensitive to the physical properties of local environment. The structure of tryptophan is shown in Fig.2. Since the aromatic indole chromophore in the tryptophan, tryptophan absorbs in the UV region, centered at 280 nm. The phosphorescence lifetime of tryptophan is sensitive to mobility of the local environment, and the probe is useful to measure motions on the millisecond time

scale in rigid environments. Since amorphous sugar glasses form a solid and rigid environment compared to liquid solution, they provide an appropriate condition for probes to have a high intense signal during phosphorescence measurements (Shah and Ludescher., 1995; McCaul and Ludescher, 1999).

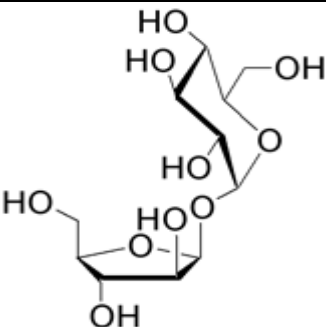
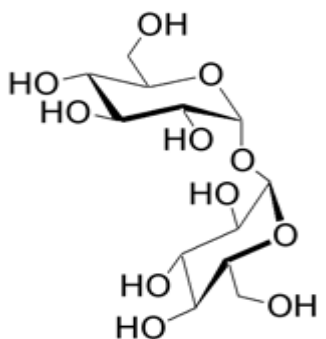
Even though tryptophan phosphorescence can provide sensitive molecular mobility information of protein in amorphous sugar matrix, a further understanding of the mechanisms governing the tryptophan triplet-state lifetimes is needed to have more accurate interpretation of this phosphorescence study (Draganski and Ludescher, 2010; Fisher et al., 2001; Gonnelli and Strambini, 2005). There are many factors, both interior and exterior, that influenced the phosphorescence lifetime of protein, like intramolecular quenching, intermolecular hydrogen-bonding effect, flexibility of the local structure. Since protein always a macromolecule, it is hard to investigate how specific groups in protein influence on tryptophan phosphorescence. Moreover, tryptophan residue in nature protein is fixed so that the signal received from tryptophan phosphorescence may not enough to understand the whole dynamic of the protein. Furthermore, it is a problem to use tryptophan phosphorescence to test protein dynamic for some nature proteins which do not have any tryptophan residue. A labeled probe in protein may disturb protein structure and property of its molecular mobility. Therefore, in many study extrinsic probes are studied as well as mutated protein with tryptophan or tryptophan analogues at the specific sites. Since complexity of protein structure and limited application of tryptophan in nature

protein and, it is much clear for us by using small triplet probes to firstly understand how tryptophan phosphorescence would be influenced by specific surrounding groups in probes as well as sugar molecules, which is useful to have better interpretation of phosphorescence results from triplet probes in protein dynamic study. 14 different small molecules containing indole group chromophore are utilized as phosphorescence probes to have a clear investigation of the above mechanisms.

By phosphorescence decay measurements, the non-radiative phosphorescence decay rates (k_{NR}) were calculated in our study to understand molecular mobility of local environment. We compare k_{NR} values of different probes here to investigate possible factors that influence tryptophan phosphorescence. In this work, the 14 small triplet probes are indole, tryptophan, the tryptophan analogues 4-fluorotryptophan, 6-fluorotryptophan, 5-bromotryptophan, 5-methyltryptophan, 5-hydroxyltryptophan, and 7-azatryptophan, two dipeptides containing tryptophan residue Trp-Gly and Gly-Trp, and the 20-residue Trp-cage protein. Generally, all those probes except 5-Br-Trp have an extreme sensitivity of the triplet excited state decay processes to the local environment. Since amorphous trehalose have more packed structure with higher T_g than amorphous sucrose, the molecular mobility in trehalose film are less influenced by temperature and more restricted than one in sucrose over the temperature range from -10 °C to 120 °C, which is observed by using all different probes in these two films. Most probes provide similar trends of the mobility in amorphous sugar film over a wide temperature range, while there are

subtle differences which could be separately caused by intramolecular quenching in Trp-Gly, heavy atom effect in 5-bromotryptophan and 4-fluoro-, 6-fluoro-tryptophan, intermolecular hydrogen-bonding effect in 7-azatryptophan and 5-hydroxyl-tryptophan.

Table 1: Chemical Structure, Glass transition Temperatures of Sucrose and Trehalose

Name	Type of glycosidic linkage and monosugar units	Chemical structure	T _g [K] at glassy state
Sucrose		α -1,2-glucos e-fructose	60-74°C [*]
Trehalose		α -1,1-glucos e-glucose	102-112°C [*]

* Here we assume that water contents (wt balance) in all amorphous sucrose and trehalose matrixes are about 0-1%. And the value of T_g[K] at glassy state is from Hancock and Dalton, 1999.

MATERIALS AND METHODS

Chemicals

All chemicals were of the highest purity grade available from commercial sources. Indole ($\geq 99\%$ pure), L-tryptophan, 5-methyl-DL-tryptophan, 5-hydroxyl-L-tryptophan ($\geq 98\%$ pure), 4-fluoro-DL-tryptophan, 6-fluoro-DL-tryptophan (98% pure), Trp-Gly, 5-bromo-DL-tryptophan (99% pure), DL-7-azatryptophan hydrate, L-tryptophanamide hydrochloride (TA; 99% pure), N-acetyl-L-tryptophan (NAT; $\geq 99\%$ pure), N-acetyl-L-tryptophanamide (NATA), Trp-Gly hydrochloride ($\geq 99\%$ pure), and D-(+)-Trehalose ($\geq 99\%$ pure) were purchased from Sigma-Aldrich. Gly-Trp and Sucrose ($\geq 99\%$ pure) were from Fisher Scientific. The structures of these molecules are showed in the Figure 2. In addition, the 20AA Trp-Cage protein (1L2Y in PDB; 98% pure) was also used as a phosphorescence probe here. And it was synthesized by United Peptide Corporation. Its structure is showed in Figure 3. These chemicals were used with no further purification. In addition, deionied water was applied in this study.

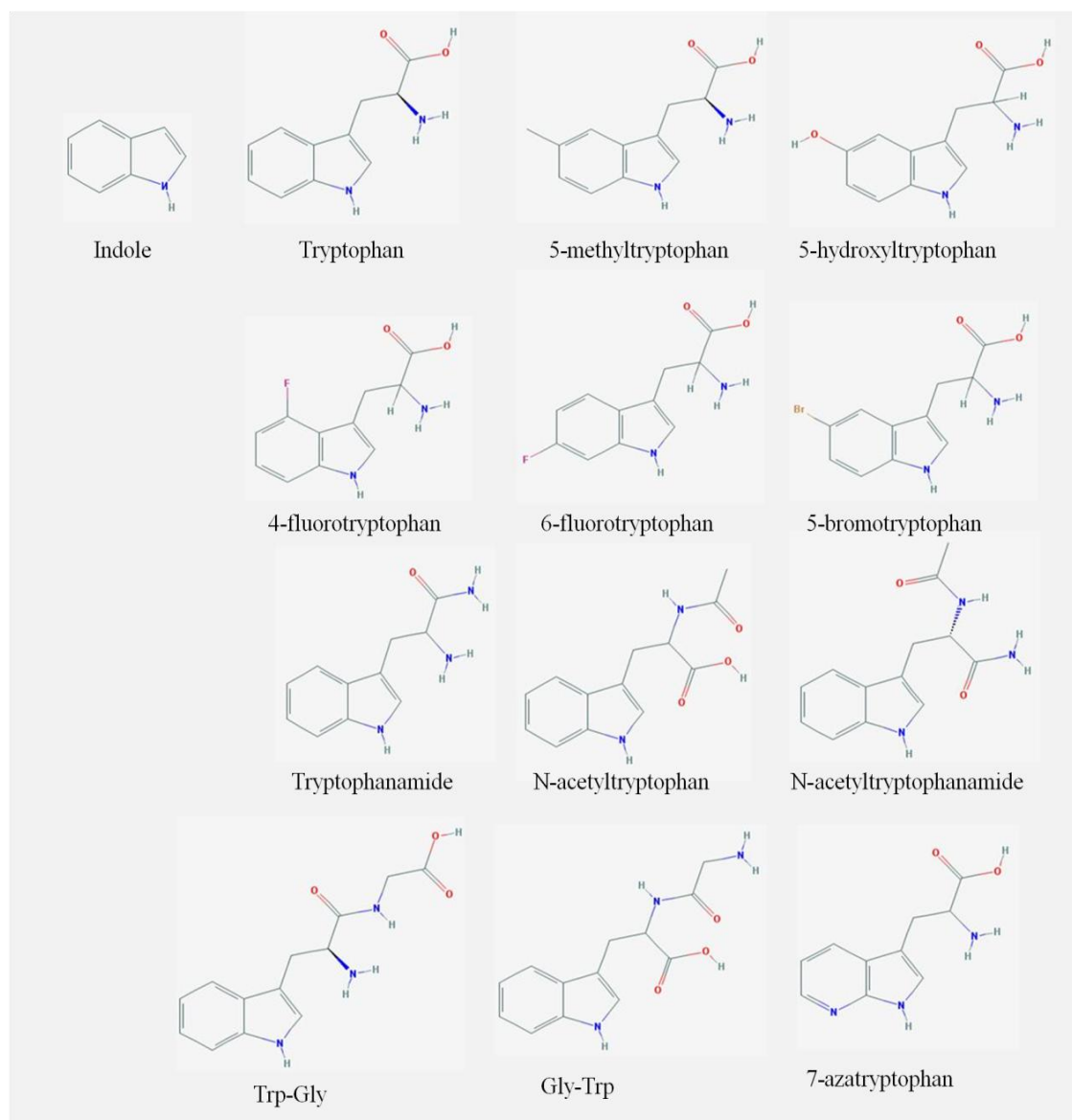


Fig. 2. Structures of the phosphorescence small molecule probes used in this study

(All of molecular structures here from <http://pubchem.ncbi.nlm.nih.gov/>)

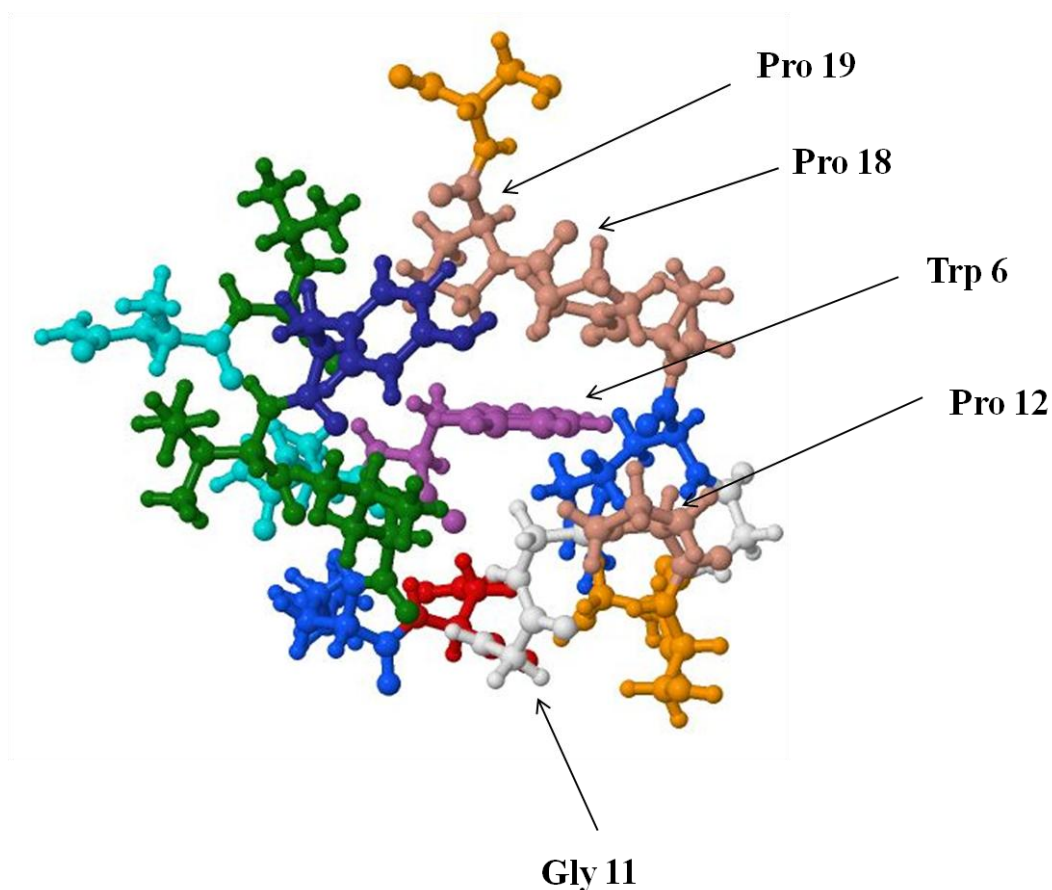


Fig. 3. Structure of 20-residue Trp-cage protein. The structure of Trp-cage protein here is from PDB (acquisition 1L2Y). And the amino acid sequence of this Trp-Cage is NLYIQ WLKDG GPSSG RPPPS. Proline residues (Pro-12, Pro-18, Pro-19) and a glycine (Gly-11) in this Trp-cage can interact together to form a compact hydrophobic core, which pack the Trp-6 side chain inside (Neidigh et al., 2002).

Sample preparation

A concentration of 65-67 wt% sucrose and a concentration of 68-70 wt% trehalose were made in water. The concentration was confirmed utilizing a refractometer (NSG precision Cells, Farmingdale, NY). Since the saturated concentration of trehalose in water is 40 wt% at 20 °C while 78 wt% at 80 °C, after solution is made it was kept in a hot water bath (~90 °C) to avoid becoming crystallized (Miller et al., 1997). All 14 of the small probes mentioned above were dissolved in deionized water. Then, an appropriate amount of probe solutions was dispersed in the concentrated sucrose or trehalose to make solutions with a mole ratio (1: 500) of probe to sugar. To produce glassy films, 7~10 µl of the solution was spread on a quartz slide (30×13.5×0.6 mm; custom made by NSG Precision Cell, Farmingdale, NY). Once spread on the slide, the film was dried under a heat gun for ~30 min and then was stored in a desiccator over P₂O₅ and Drierite. Films were stored for at least one week before any phosphorescence measurement. Here, we assume that water content is about 0%-1% by weight due to the extensive equilibration time and the thinness of the film (You and Ludescher, 2008).

Luminescence Measurement

Fluorescence and phosphorescence spectra were measured using a Cary Eclipse fluorescence spectrophotometer (Varian instruments, Walnut Creek, CA). Absorption spectra of the above probes were collected in amorphous trehalose films at 20 °C. For fluorescence excitation, data was collected from 230 nm to 320 nm (5 nm bandwidth)

with emission wavelength of 350 nm (20 nm bandwidth). For phosphorescence excitation, data is collected from 230 nm to 350 nm (20 nm bandwidth) with emission wavelength 440 nm (20 nm bandwidth). At the same time, phosphorescence and fluorescence emission spectra of probes were collected in amorphous trehalose film at 20 °C. For fluorescence emission, data was collected from 300 nm to 500 nm (5 nm bandwidth) with excitation wavelength 280 nm (20 nm bandwidth). For phosphorescence emission, data was collected from 380 nm to 550 nm (20 nm bandwidth) with excitation wavelength 280 nm (20 nm bandwidth). For phosphorescence excitation and emission measurements, all samples were flushed for at least 30 min with N₂ gas containing < 1ppm of residual O₂ to eliminate O₂ which effectively quenches the triplet state, while for fluorescence excitation and emission spectra, N₂ was not needed to flush samples.

Phosphorescence decays in amorphous films were also measured using a Cary Eclipse fluorescence spectrophotometer (Varian instruments, Walnut Creek, CA). This instrument uses a high-intensity pulsed lamp and collects intensity in analogue mode; data were not collected within the first 0.2 ms to suppress fluorescence coincident with the lamp pulse. Because of phosphorescence measurements, all samples were flushed with N₂ to eliminate O₂ which effectively quenches the triplet state. All measurements were made in quadruplicate at least. Sample temperature of the cuvette holder was controlled using either a thermoelectric heater/cooler (Varian Instrument) or a water bath (Fisher Scientific, Pittsburgh, PA).

For phosphorescence lifetime measurements as a function of temperature, samples were excited at 280 nm (20 nm bandwidth) and their emission transients were collected at 440 nm (20nm bandwidth) over the temperature range from -10 °C to 90~120 °C with an initial delay of 0.2 ms. For getting maximum information from samples as this machine can do, the gate time is one thousandth of the decay time. Since the amorphous sugar matrix is dynamically heterogeneous on the molecular level, multi-exponential functions were applied to fit the phosphorescence intensity decay. The multi-exponential model is as show in Equation 1. In this study, five exponential fits are applied to all the decays of probes. The τ_i are decay times, and the α_i represent the amplitudes of the components at time zero and n is the number of decay times. Phosphorescence lifetimes were determined using the statistical fitting program Igor (Wavemetrics, Inc., Lake Oswego, OR). Fits were judged satisfactory if the R^2 values were in the range of 0.995-1.0 and the modified residuals $((\text{data-fit})/\text{data}^{1/2})$ varied randomly about zero. The average lifetime was calculated using Equation 2.

$$I(t) = \sum_{i=1}^n \alpha_i \exp(-t / \tau_i) \quad (1)$$

$$\overline{\tau_p} = \frac{\sum_{i=1}^n \alpha_i \tau_i}{\sum_{i=1}^n \alpha_i} \quad (2)$$

The phosphorescence lifetime τ_p is directly related to the rate constant for de-excitation of the triplet excited state of the probe according to equation 3. In this equation, k_{RP} is the rate of radiative decay to the ground singlet state, and k_{NR} is the rate of non-radiative decay to the singlet state followed by vibrational relaxation to ground state due to collisional quenching. The radiative decay rate (k_{RP}) can be determined from measurements of lifetime in organic glasses at low temperature where non-radiative rates are negligible. Here, we assume that there is no collisional quenching by oxygen under nitrogen flushing during measurements and the self-quenching due to collisions between probes is negligible within the extremely viscous amorphous solid.

$$\bar{\tau}_p = (k_{RP} + k_{NR}(T))^{-1} \quad (3)$$

The non-radiative decay rate can be calculated using equation 3 since k_{RP} can be measured at low temperature. The temperature dependence of k_{NR} is plotted using an Arrhenius analysis (equation 4). At the same time, activation energy (E_a) for the motions giving rise to non-radiative decay can be calculated by this equation.

$$\ln k_{NR} = \ln k_{NR}^0 - \frac{\Delta E_a}{R} * \frac{1}{T} \quad (4)$$

RESULTS AND DISCUSSION

1. Excitation and Emission Spectra of Luminescence for Probes in Amorphous Sugar Matrix.

1.1 Luminescence Excitation Spectra

Fluorescence and phosphorescence excitation spectra of indole, tryptophan, and the other 11 probes in the trehalose matrix are showed in Fig.4 and Fig.5. The absorphance of Indole, TA, NAT, NATA, 5-methyl-Trp, 6-F-Trp, Trp-Gly, and 20-residue Trp-cage protein are not shifted from that of tryptophan. Yet, 7-azatryptophan and 5-hydroxyltryptophan have red shifted excitation spectra and 4-F-Trp has a blue-shifted excitation in relation to tryptophan. Since 4-fluorotryptophan was not very detectable on fluorescence spectra (both excitation and emission), only phosphorescence spectra data of this probe is provided here. Because of red shifted excitation spectra, 7-azatryptophan and 5-hydroxyltryptophan allow selective photoexcitation. Hence, they are commonly applied in protein studies as tryptophan analogs.

1.2 Luminescence Emission Spectra

The fluorescence and phosphorescence emission spectra for those probes were all collected at 20 °C with excitation wavelength at 280 nm (Fig.4 and Fig.5). NAT, NATA, and 4-F-Trp (only phosphorescence emission is provided here) are markedly red-shifted (about 4-6 nm); 5-OH-Trp and 6-F-Trp are about 8-12 nm red-shifted from that of tryptophan. Moreover, 7-azatryptophan has the largest red-shifted (about

32-40 nm) emission from that of tryptophan in both fluorescence and phosphorescence emission spectra than another probes.

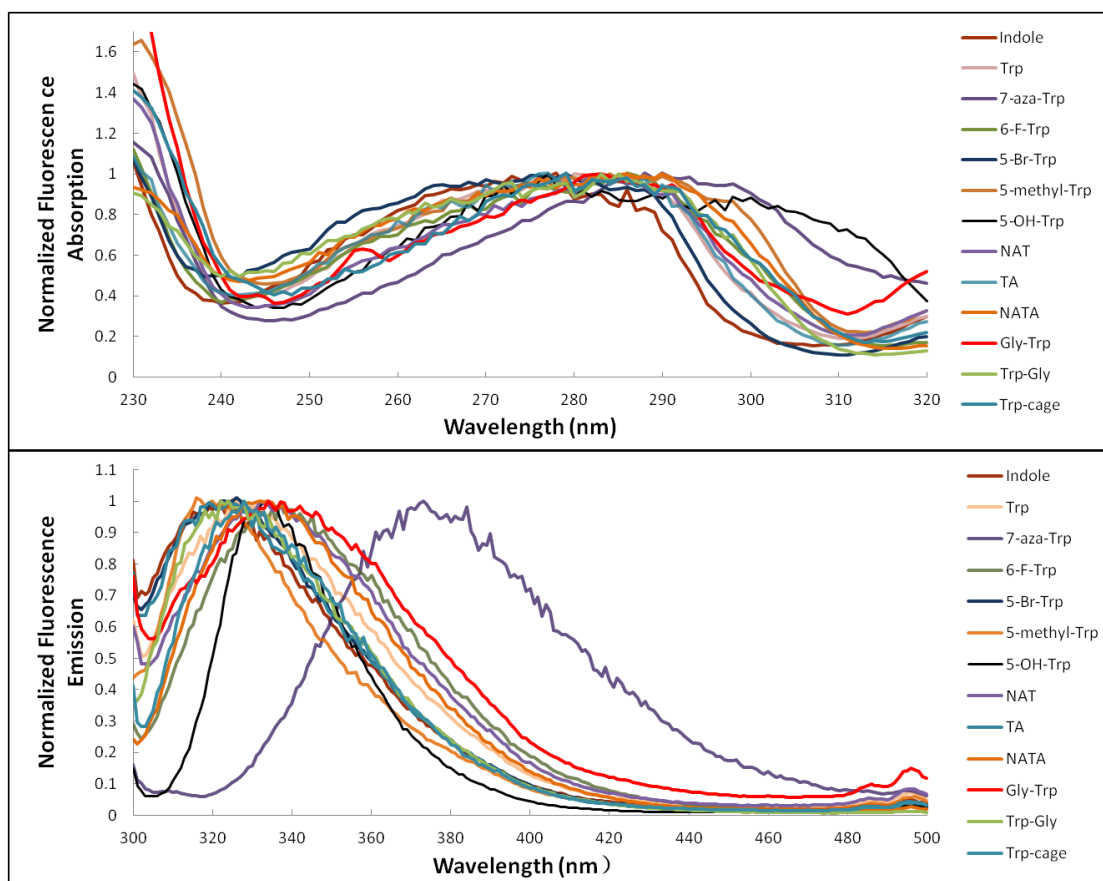


Fig. 4. Normalized fluorescence excitation and emission spectra of some probes (Indole, Trp, 7-aza-Trp, 6-F-Trp, 5-Br-Trp, 5-methyl-Trp, 5-OH-Trp, NAT, TA, NATA, Trp-Gly, Gly-Trp, and 20-residue Trp-cage protein) in trehalose with $\lambda_{\text{ex}} = 280$ nm for emission spectra and with $\lambda_{\text{em}} = 350$ nm for excitation spectra at 20 °C.

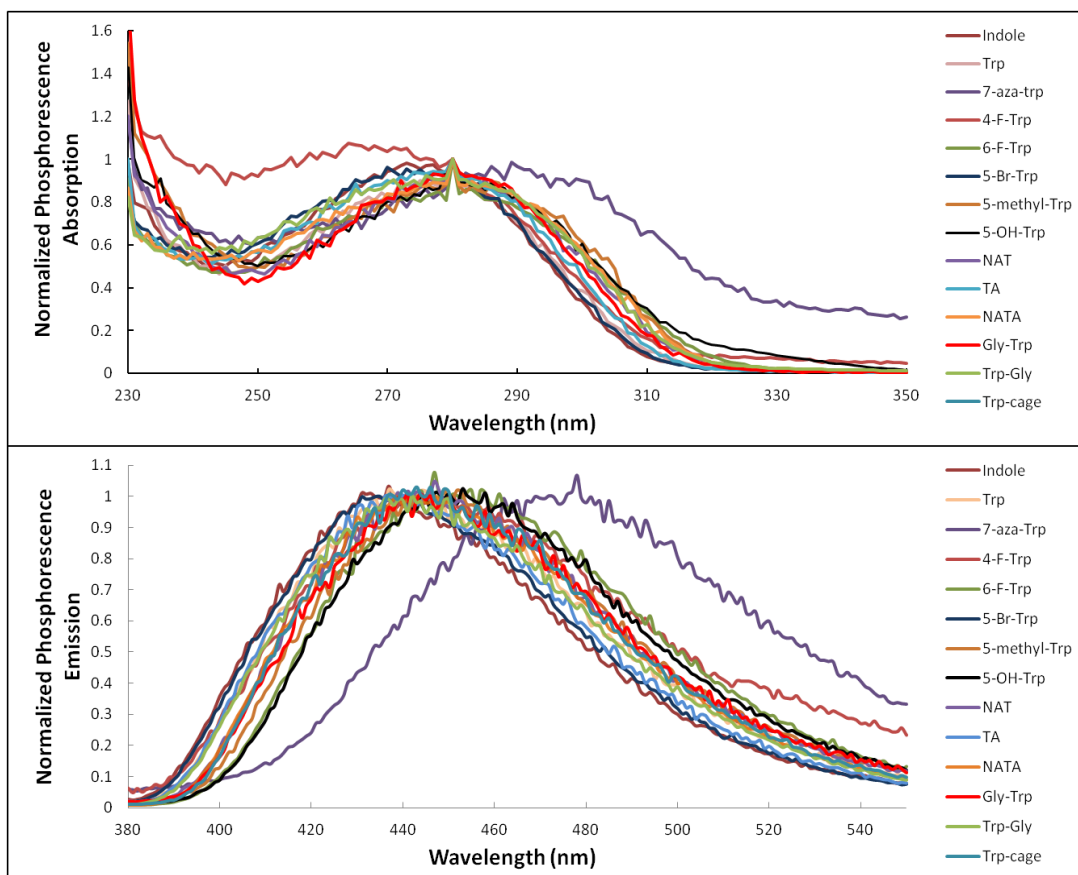


Fig. 5. Normalized phosphorescence excitation and emission spectra of some probes (Indole, Trp, 7-aza-Trp, 4-F-Trp, 6-F-Trp, 5-Br-Trp, 5-methyl-Trp, 5-OH-Trp, NAT, TA, NATA , Trp-Gly, Gly-Trp, and 20-residue Trp-cage protein) in amorphous trehalose with $\lambda_{\text{ex}} = 280$ nm for emission spectra and with $\lambda_{\text{em}} = 440$ nm for excitation spectra at 20 °C.

2. Phosphorescence Intensity Decay

The phosphorescence decay of indole, tryptophan, tryptophan analogs, and two dipeptides with tryptophan residues in amorphous sucrose and trehalose were well-fitted to five-exponential decay function over the temperature range from -10 °C to 90~120 °C. All of probes were excited at 280 nm and their emission collected at 440 nm. Fits were judged satisfactory if the modified residuals $((\text{data-fit})/\text{data})^{1/2}$ varied randomly about zero. The normalized phosphorescence intensity decays of some probes, indole, tryptophan, 5-Br-Trp, 5-hydroxytryptophan, NATA, Gly-Trp and Trp-cage protein in amorphous trehalose films at 20 °C are plotted in the Fig. 6 as well as in Fig. 7 (Intensity is in logarithmic scale). From inspection of these two figures, the overall rate of intensity decay from fast to slow is 5-Br-Trp > indole > 5-OH-Trp > tryptophan ~ Trp-cage protein > NATA \geq Gly-Trp. Generally, the slower the intensity decrease, the longer lifetime the probe in the matrix has. Therefore, the probe, Gly-Trp, in amorphous trehalose matrix has the most rigid local environment.

All of phosphorescence intensity decays were fitted to the 5-exponential function in equation 1. In the Fig. 8, the original phosphorescence decay data of Trp-cage protein in amorphous trehalose matrix was plotted as well as the fit curves using the different exponential functions (1-, 2-, 3-, 4-, 5- and 6- exponential functions). The quality of these fits was indicated by the modified residuals corresponding to each of them. The modified residuals vary more and more randomly when we used these

functions with exponential number from 1 to 5 (Fig.9). Once the exponential number is up to 6, the modified residual has already similar to modified residual of 5-exponential function (Fig.9). And 5-exponential function was complicated enough to describe the intensity decays for probes in amorphous solids.

The plots of each lifetime component for Trp-cage protein as a function of temperature are shown in Fig. 10. The amplitude of each lifetime component for Trp-cage protein as a function of temperature is shown in Fig. 11. Fig. 12 shows amplitude the distribution as a function of each lifetime component for Trp-cage protein over the temperature range from -10 °C to 110 °C. Generally, as temperature increased the amplitudes of longer lifetime components (e.g. τ_5) decreased while the amplitudes of the shorter lifetime components (e.g. τ_1) increased. In the other word, amorphous solids have heterogeneous structure so that molecules have different local environment with different mobile properties. As the temperature increase, the ratio of molecules in the rigid local environment becomes smaller while the ratio of molecules in the mobile local environment becomes larger.

The average lifetime at each temperature was calculated using Eq. 2. The total rate constant of phosphorescence radiative decay, k_p , and non-radiative decay, k_{NR} , is equal to the inverse of the average lifetime. The total decay rate is the sum of the k_{RP} and k_{NR} . The k_{RP} values were determined by measurements of the phosphorescence decay at the low temperature (77K), at which temperature k_{NR} are negligible so that

k_{RP} is equal to the inverse of the phosphorescence lifetime. We assume that probes, including TA, NAT, NATA, 5-methyltryptophan, Trp-Gly, Gly-Trp, Trp-cage protein, have the same phosphorescence decay rate as tryptophan, $0.167s^{-1}$. And the phosphorescence decay rates (k_{RP}) of 5-OH-Trp applied here is $0.293s^{-1}$ and k_{RP} of 7-azaTrp is $3.22s^{-1}$ (Sengupta et al., 2002). Through applying average lifetime and constant k_{RP} of each probe above, the k_{NR} value is calculated through equation 3. The decrease lifetime as a function of temperature corresponds to an increase with temperature in the non-radiative decay rate k_{NR} (Equation 3). Lower k_{NR} indicates more rigid matrix with less molecular collision and quenching for the probe; higher k_{NR} indicates more mobile matrix with high possibility of molecular collision and quenching for the probe.

A plot of $\ln(k_{NR})$ as a function of temperature is shown in Fig. 13 from the data of Trp-cage protein in amorphous trehalose matrix. The $\ln(k_{NR})$ value of Trp-cage protein is in the range of -0.12 at -10 °C to 6.48 at 120 °C, which indicates a large fold difference in average mobility. Also, we can also apply arrhenius plots of $\log(k_{NR})$ for average lifetime of probes as a function of temperature, which are showed in the following sections. Here, through plots of $\ln(k_{NR})$ versus T in Fig.13, activation energy were calculated by Equation 4. Three close data points were chose to get the linear trend line with linear equation. The slope of this linear equation is $(-E_a/R)$ corresponding to equation 4. The activation energy calculated here is supposed to the activation energy at temperature of the middle data point. For example, from the

equation A in Fig. 13, the slope is -5347.3 so that the activation energy at 30 °C is about 44.46 kJ/mol. The plot of activation energy as a function of temperature from 0 °C to 110 °C is showed in Fig. 14. for Trp-cage protein in amorphous trehalose film. Dranca has reported that the activation energy for trehalose at 60 °C was 75kJ/mol, and for sucrose at 20 °C was 42kJ/mol, which were comparable to our results by phosphorescence of different probes (Dranca et al., 2009).

Fig. 15 and Fig. 16 are the Arrhenius plots of $\log(k_{NR}/s^{-1})$ versus K/T for 12 probes both in amorphous sucrose and trehalose (11 probes from my own results including indole, tryptophan, TA, NAT, NATA, 5-methyl-Trp, 5-OH-Trp, 7-Aza-Trp, Trp-Gly, Gly-Trp and Trp-cage protein; results of HSA from my labmate Andrew Draganski). Gly-Trp and NATA both in amorphous sucrose and trehalose are the most rigid among these 12 probes. Then the k_{NR} value of tryptophan, TA, NAT, Trp-Gly, 5-methyl-Trp and Trp-cage protein are very close in glassy trehalose film with the temperature range from -10 °C to 120 °C. Moreover, in amorphous sucrose, the k_{NR} value of TA, NAT, 5-methyl-Trp and Trp-Gly are still similar to each other over the temperature range from -10 °C to 90 °C, while tryptophan and Trp-cage protein start to have a higher k_{NR} than the former 4 probes when temperature above 20 °C. After the above probes, the less rigid probes in amorphous trehalose (k_{NR} value from smaller to larger, namely molecule mobility from rigid to mobile) are 5-OH-Trp, indole, HSA and then 7-Aza-Trp.

In sucrose, the difference among k_{NR} trends of all probes here varies much larger than one in trehalose. The plots of the activation energy as a function of temperature was showed for some selected probes in amorphous sucrose (Fig. 17) as well as in amorphous trehalose (Fig. 18). In the glassy trehalose with T_g at about 110 °C, these probes indicates the similar activation energy over the temperature range from 0 °C to 90 °C (Fig. 17). Only indole shows a little higher activation energy at the low temperature, and HSA shows a little lower activation energy at the high temperature. But, in amorphous sucrose with T_g at about 60 °C, a broad distribution of the activation energy values was depicted for these probes in the temperature between 10 °C to 50 °C (Fig. 18). Generally, in amorphous sucrose matrix, activation energy from high to low for these probes at the temperature between 10 °C to 40 °C are tryptophan, Trp-cage > TA, NAT, Trp-Gly, Gly-Trp, 5-methyl-Trp, 7-Aza-Trp, indole > 5-OH-Trp > NATA > HSA. The molecular mobility of HSA in local environment of amorphous sucrose is less influenced by glass transition temperature than the others here. In all, the response from probes in sucrose to the thermodynamic in the local environment is much more variety than one from probes in trehalose, which is probably caused by the nature properties of these two disaccharides.

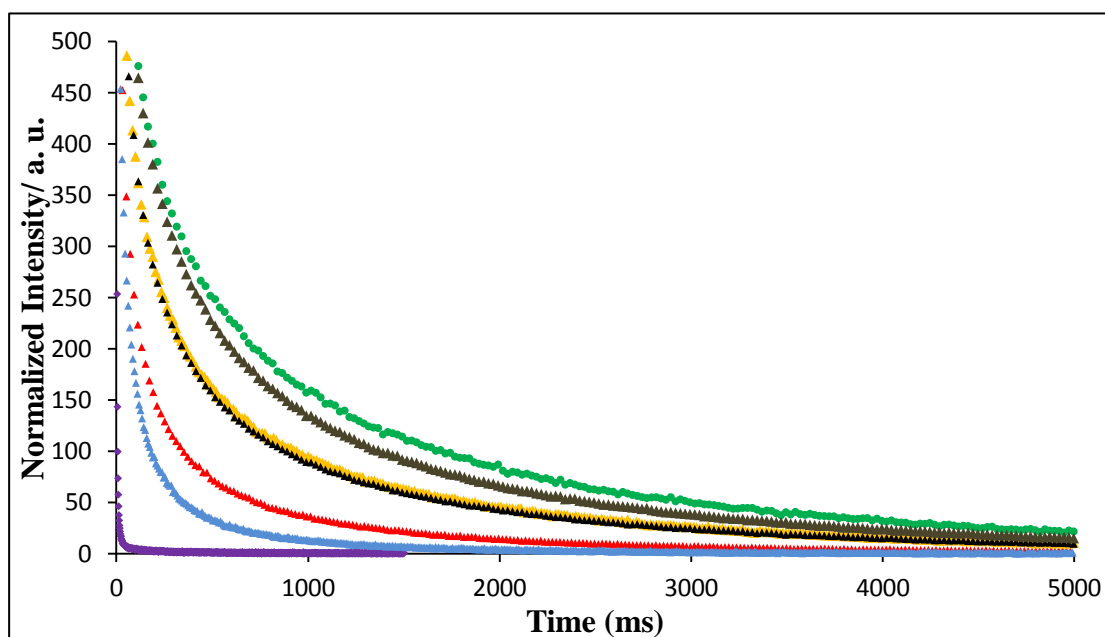


Fig.6. Normalized phosphorescence intensity decay versus time for various probes in amorphous trehalose film at 20 °C, including indole, tryptophan, 5-Br-Trp, 5-OH-Trp, NATA, Gly-Trp and Trp-cage protein. Purple: 5-Br-Trp; Blue: indole; Red: 5-OH-Trp; Black: tryptophan; Yellow: 20-residues Trp-cage protein; Gray: NATA; Green: Gly-Trp.

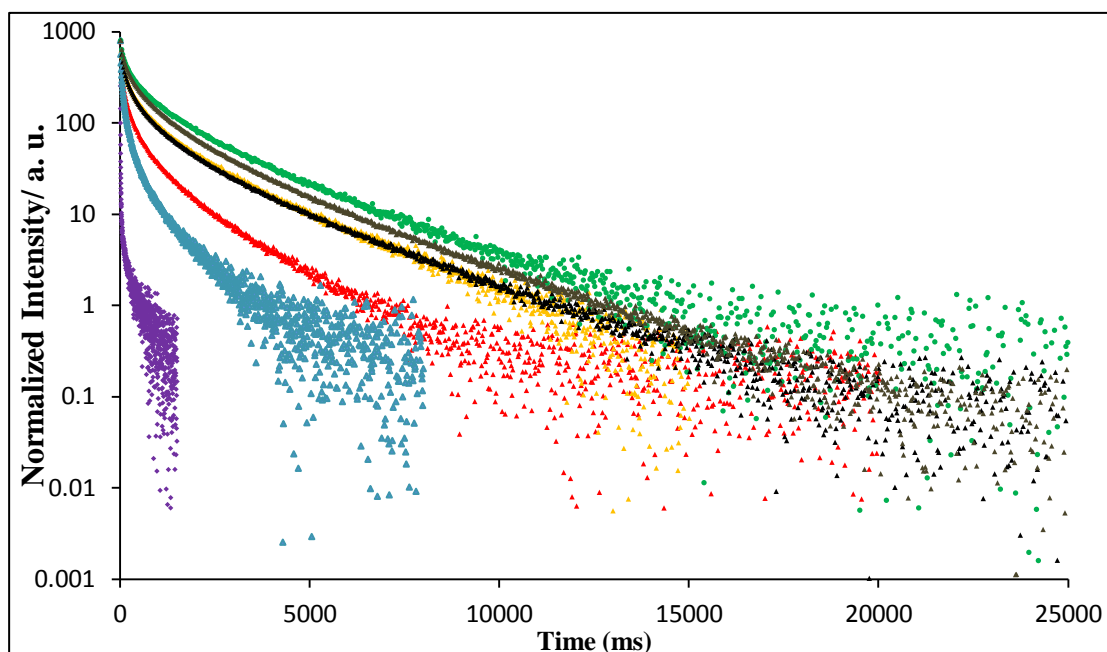


Fig.7. Normalized intensity in logarithmic scale versus time for various probes in amorphous trehalose at 20 °C, including indole, tryptophan, 5-Br-Trp, 5-OH-Trp, NATA, Gly-Trp and Trp-cage protein. Purple: 5-Br-Trp; Blue: indole; Red: 5-OH-Trp; Black: tryptophan; Yellow: 20-residues Trp-cage protein; Gray: NATA; Green: Gly-Trp.

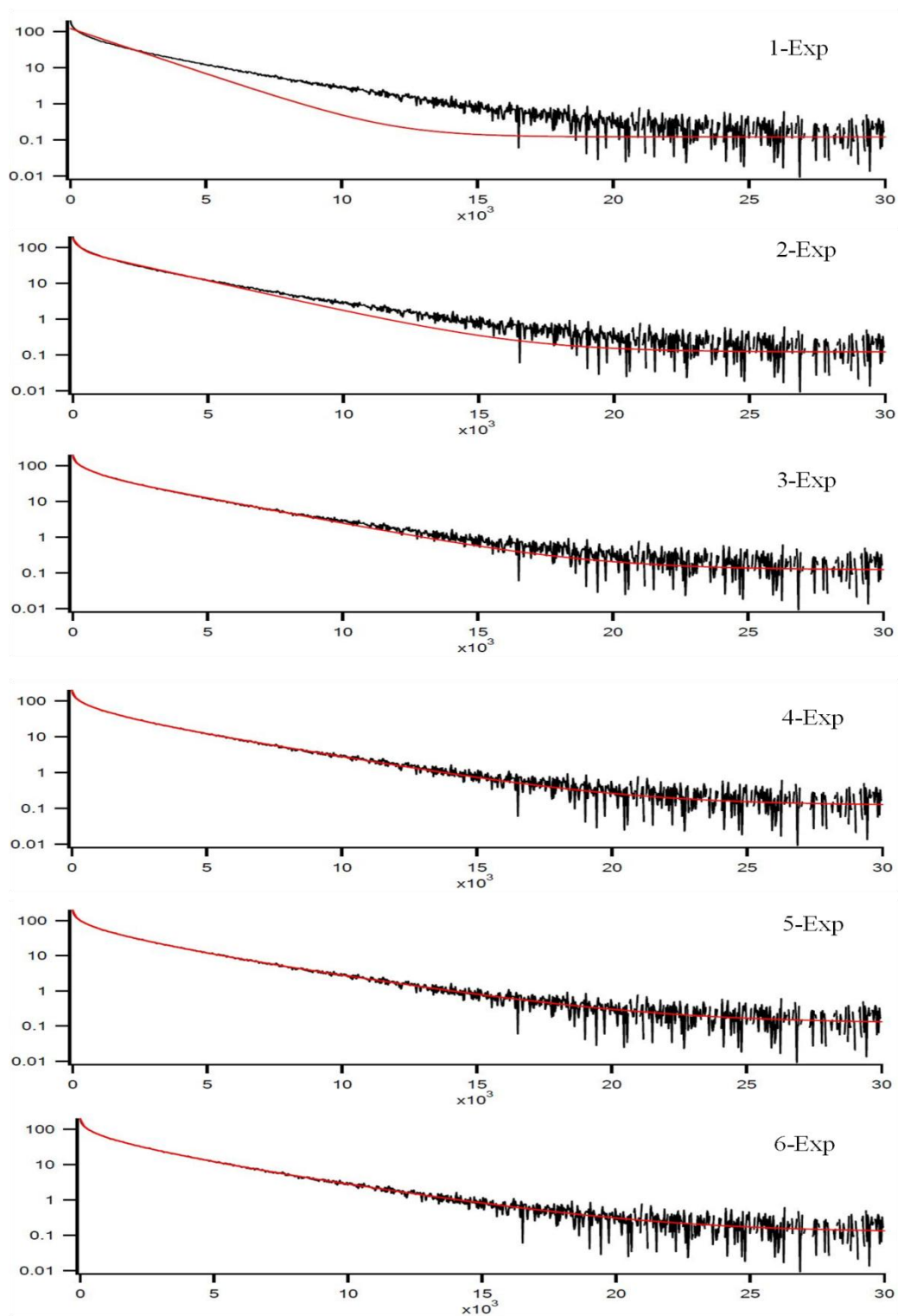


Fig.8. Phosphorescence intensity decays of Trp-cage protein in amorphous trehalose film at $-10\text{ }^{\circ}\text{C}$. Black lines: raw data; Red curves: the fit curves using multi-exponential functions, including 1-Exp, 2-Exp, 3-Exp, 4-Exp, 5-Exp, and 6-Exp functions (Equation 1).

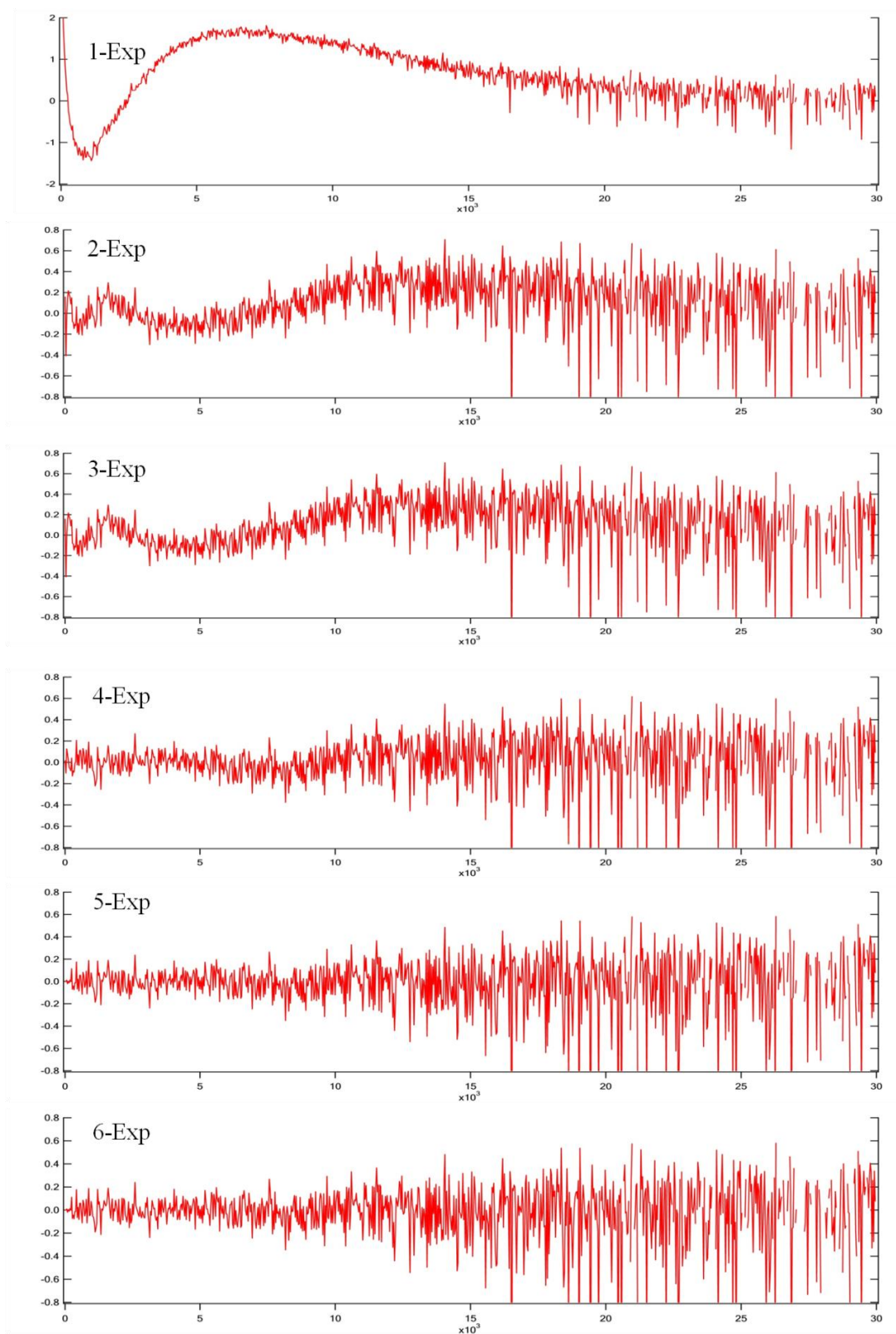


Fig.9. Modified residuals ($((\text{data-fit})/\text{data})^{1/2}$) versus time for Trp-cage protein in amorphous trehalose film at $-10\text{ }^{\circ}\text{C}$. Red curves: modified residuals corresponding to 1-Exp, 2-Exp, 3-Exp, 4-Exp, 5-Exp, and 6-Exp functions.

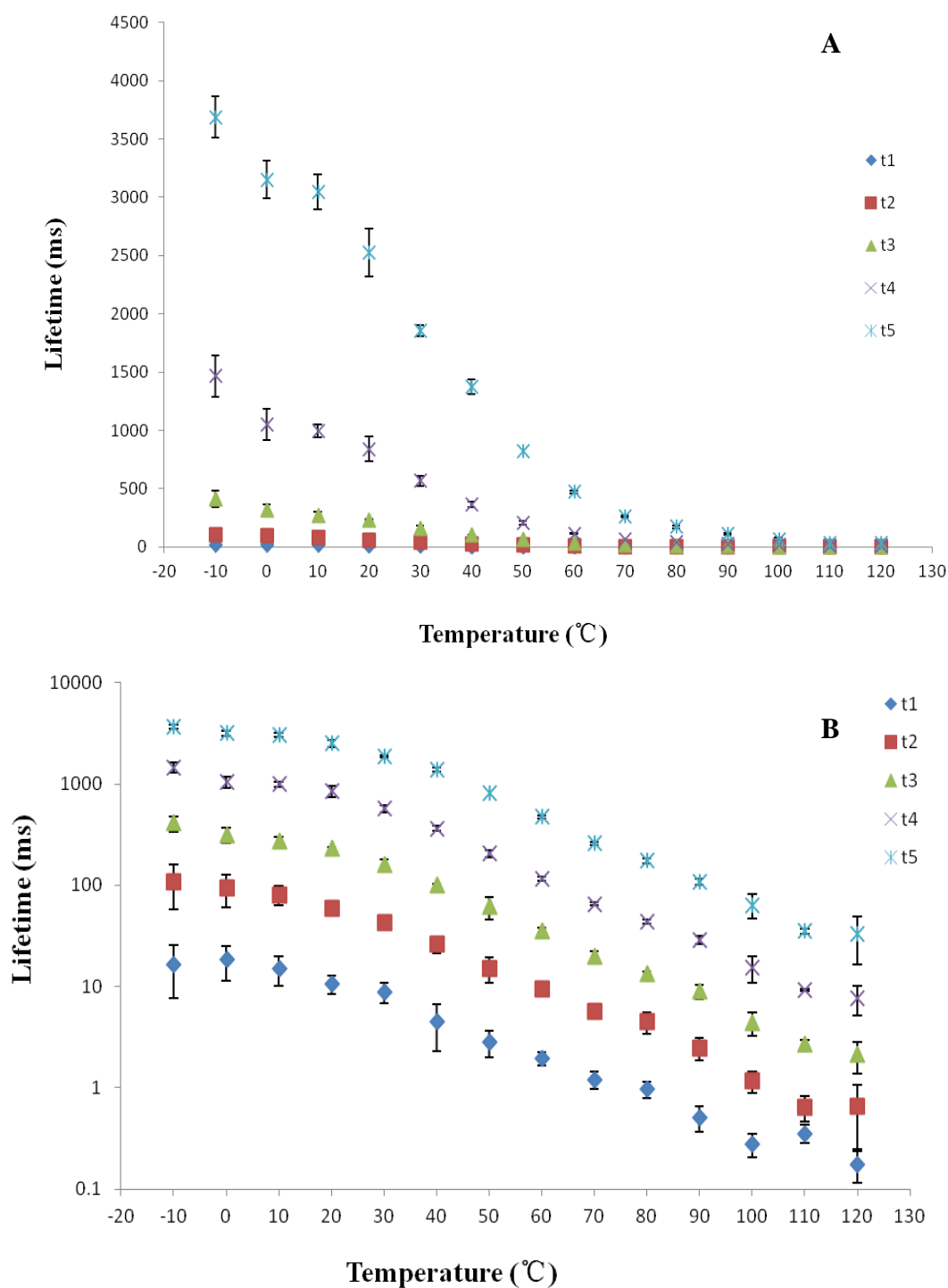


Fig.10. Lifetime (τ_i) versus temperature of Trp-cage in amorphous trehalose film.

The data were taken every 10 °C from -10 °C to 120 °C. In B, the lifetime axis is in logarithmic scale.

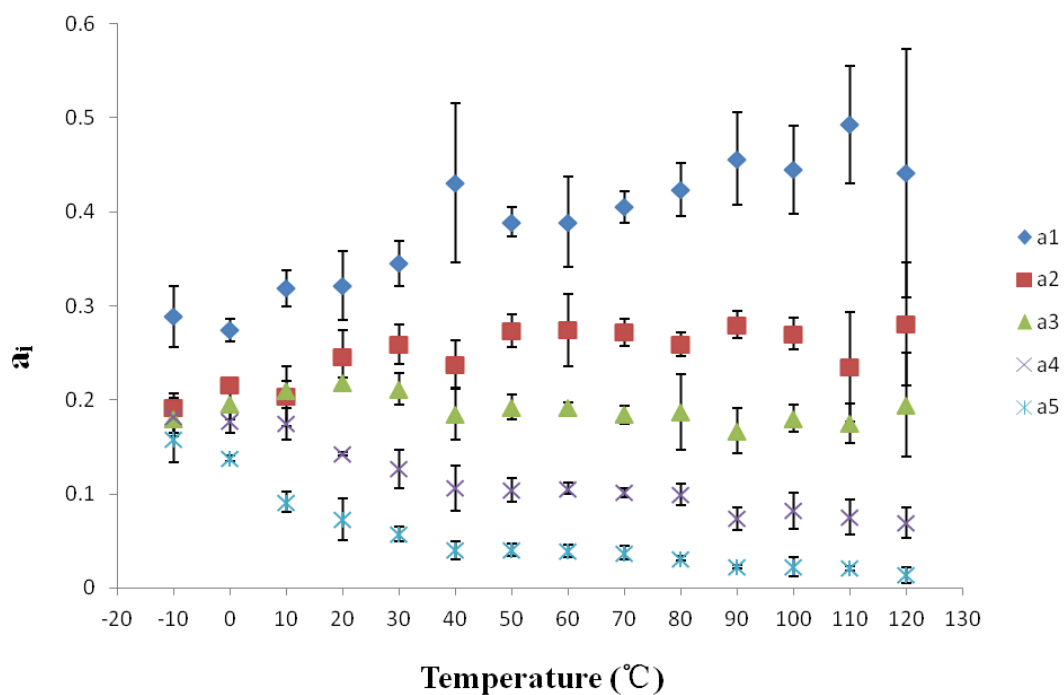


Fig.11. Amplitude (a_i) versus temperature of Trp-cage protein in amorphous trehalose film. The data were taken every 10 °C over the temperature range from -10 °C to 120 °C.

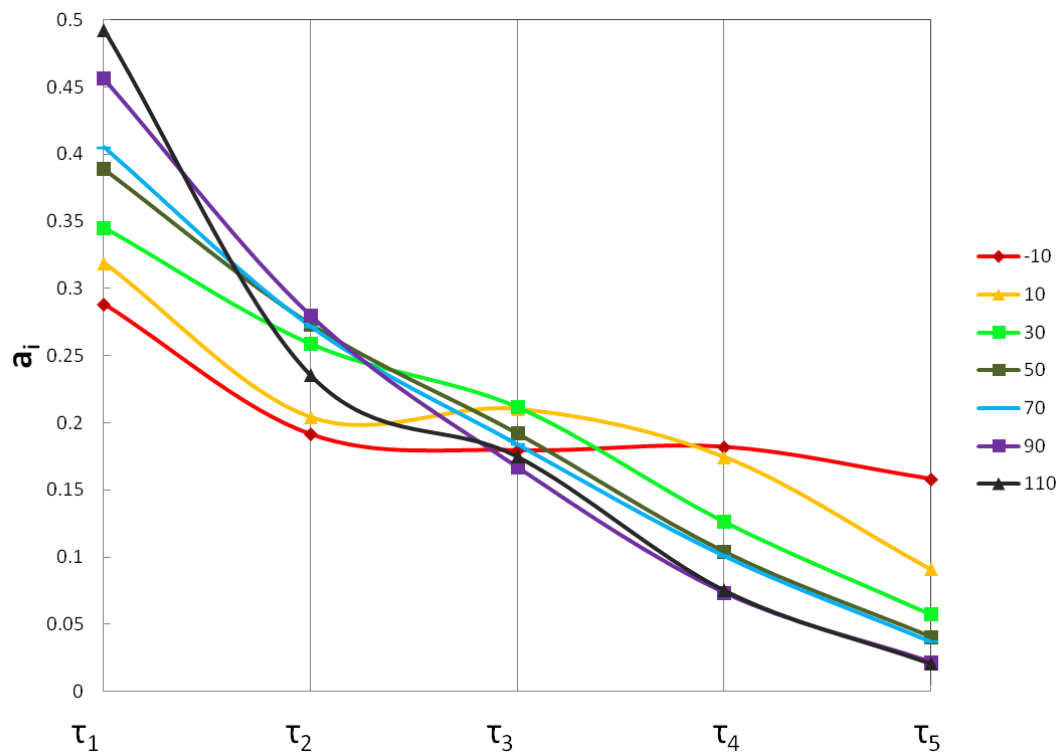


Fig.12. Amplitude (a_i) at corresponding decay time (τ_i) of Trp-cage protein in amorphous trehalose film. The lifetime sequence from shorter to longer is τ_1 , τ_2 , τ_3 , τ_4 and τ_5 .

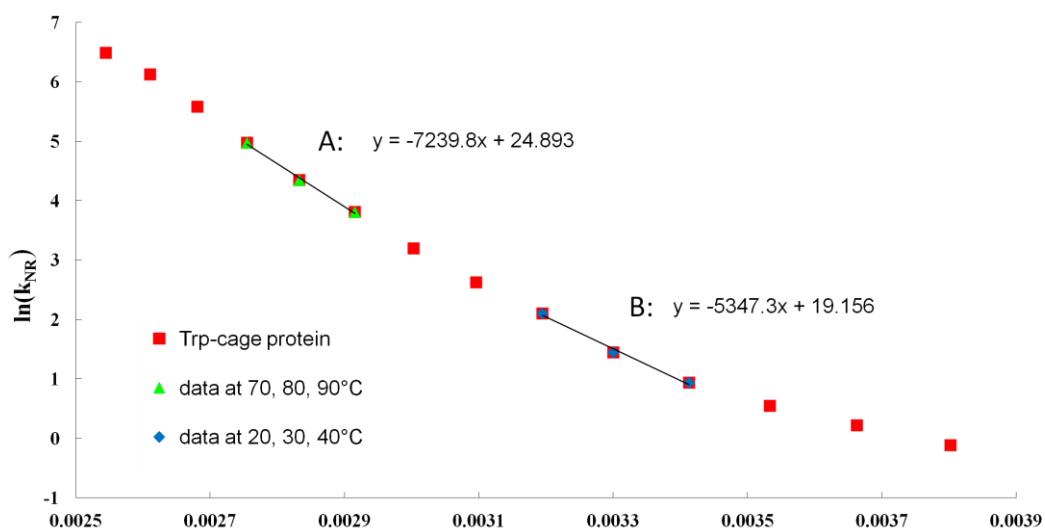


Fig.13. Average lifetimes as a function of temperature for Trp-cage protein in amorphous trehalose film. Red square data points are the $\ln(k_{NR})$ values for Trp-cage in amorphous trehalose from -10 °C to 120 °C. The data here were measured every 10 °C. Green data points are the $\ln(k_{NR})$ values for Trp-cage protein in amorphous trehalose at 70 °C, 80 °C and 90 °C. Blue data points are the $\ln(k_{NR})$ values for Trp-cage protein in amorphous trehalose at 20 °C, 30 °C and 40 °C. Equation A corresponds to the trend line of the green triangle data points. And equation B is from the trendline of the blue rhombus data points.

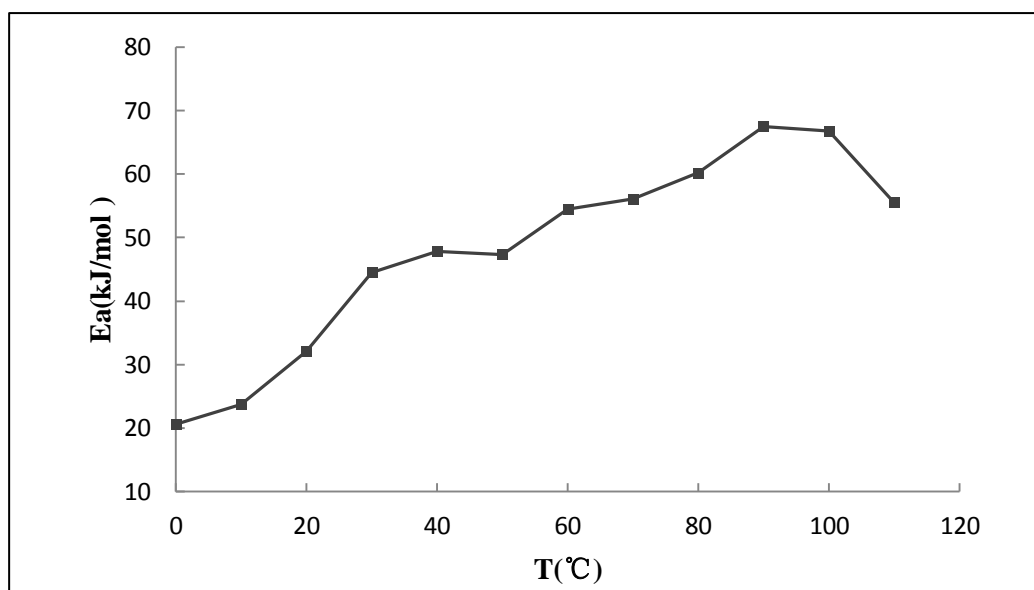


Fig. 14. The activation energy as a function of temperature for Trp-cage protein in amorphous trehalose film.

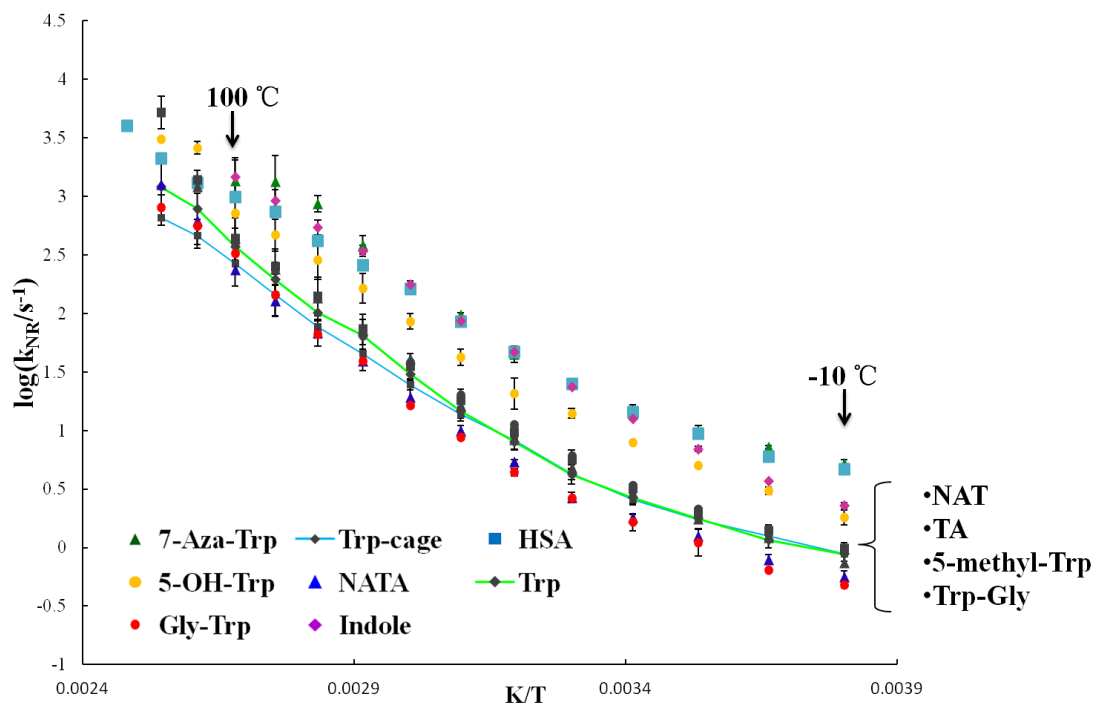


Fig. 15. $\log(k_{NR}/s^{-1})$ versus K/T in amorphous trehalose film for 12 probes including indole, Trp, TA, NAT, NATA, 5-methyl-Trp, 7-Aza-Trp, 5-OH-Trp, Trp-Gly, Gly-Trp, Trp-cage protein, and HSA. The data for these probes in trehalose were measured every 10 °C from -10 °C to 120~130 °C. The gray dots except Trp (with green line) and Trp-cage protein (with blue line) are TA, NAT, 5-methyl-Trp and Trp-Gly.

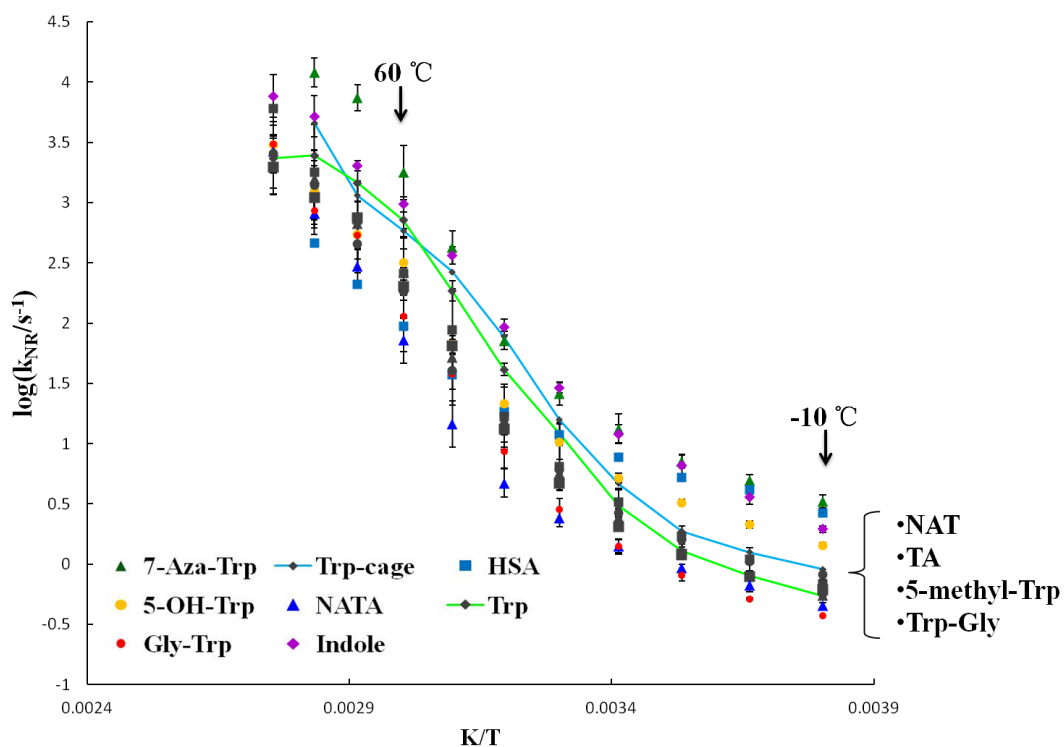


Fig. 16. $\log(k_{NR}/s^{-1})$ versus K/T in amorphous sucrose film for 12 probes including indole, Trp, TA, NAT, NATA, 5-methyl-Trp, 5-OH-Trp, 7-Aza-Trp, Trp-Gly, Gly-Trp, Trp-cage protein, and HSA. The data for these probes in sucrose were measured every 10 °C from -10 °C to 80~90 °C. The gray dots except Trp (with green line) and Trp-cage (with blue line) are TA, NAT, 5-methyl-Trp and Trp-Gly.

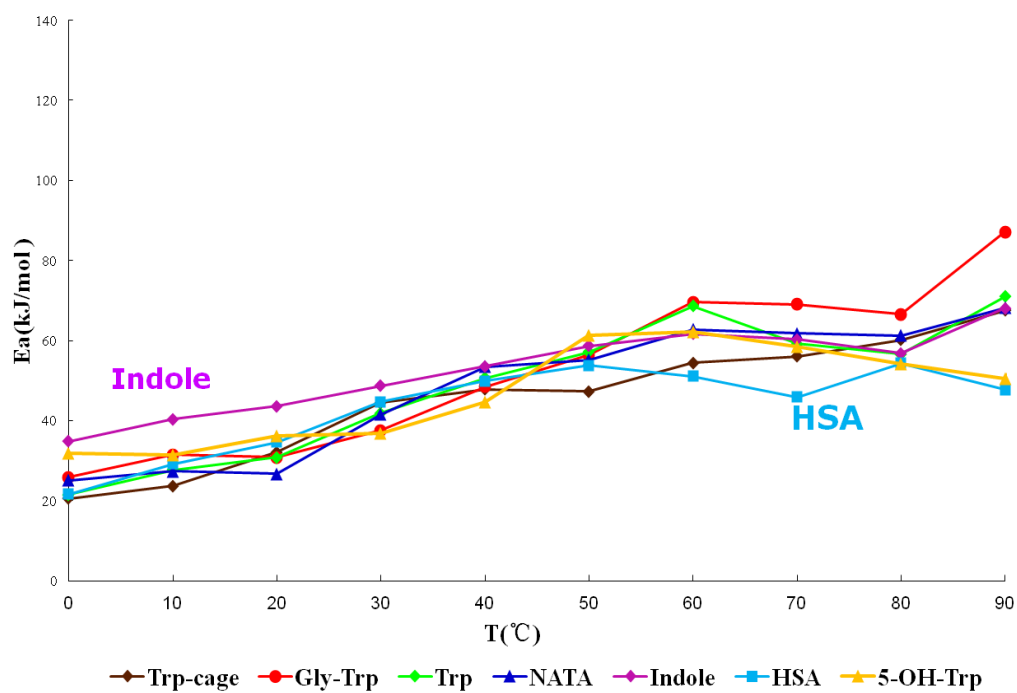


Fig. 17. Activation energy versus $T/^{\circ}\text{C}$ in amorphous trehalose film for selected probes including indole, Trp, 5-OH-Trp, NATA, Gly-Trp, Trp-cage protein and HSA.

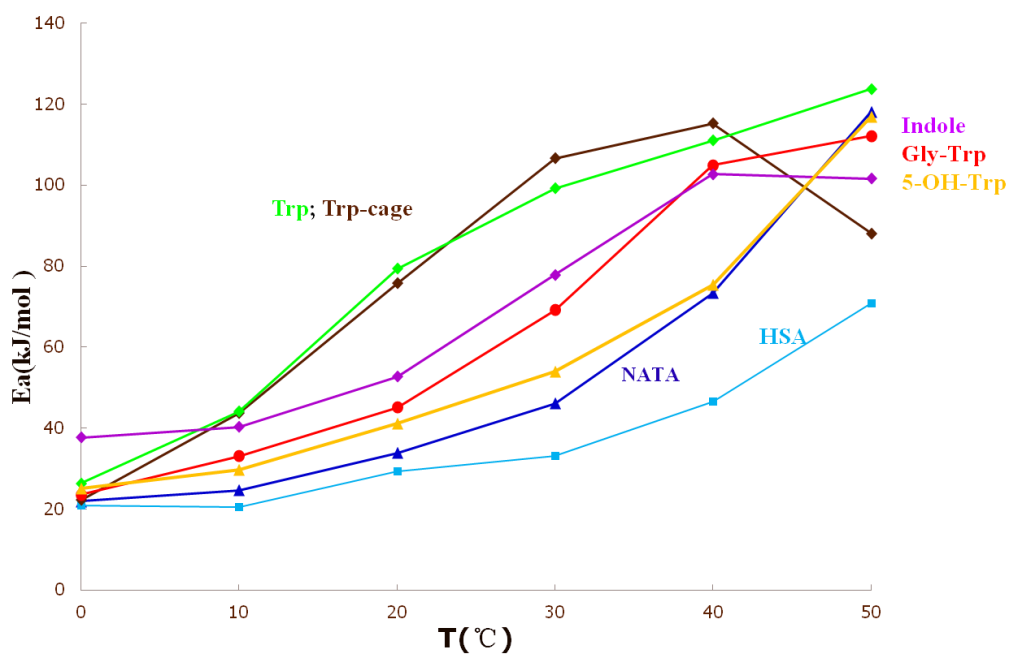


Fig. 18. Activation energy versus $T/^{\circ}\text{C}$ in amorphous sucrose film for selected probes including indole, Trp, 5-OH-Trp, NATA, Gly-Trp, Trp-cage protein and HSA.

3. Variation of Phosphorescence Non-radiative Decay Rate (k_{NR}) and Activation Energy (E_a) in Amorphous Sucrose and Trehalose

During the last decade, many researches and applications utilized amorphous solids in pharmaceutical to store active ingredients which have poor aqueous solubility, or/and to protect functionality of susceptible compositions (Hancock and Zografi, 1997; Pouton, 2006; Wang, 1999). And saccharides are typically material to be utilized as a cryoprotectant, lyoprotectant and matrix for amorphous drugs (shambling et al., 1999; Crowe, 1998). For example, protein stability in amorphous solids can be improved by the inclusion of sugar molecules during freeze-drying. In addition, some organisms can produce sugars to protect themselves against extreme dry condition. Nowadays, this bioprotection by amorphous sugars to protein at molecular level is still not very clear even with many proposed hypotheses (Longo et al., 2010). Therefore, the study on amorphous sugars is still needed to provide more information on molecular mechanism of the relaxation processes in the carbohydrates.

Since the complexity of saccharides, it is necessary to investigate the dynamical properties of the simplest systems (like mono- and disaccharides) at first in order to understand the behavior of the more complicated carbohydrates. Among disaccharides, trehalose is accumulated in certain spores, yeasts, and microscopic animals, whereas sucrose exists in some pollen, plant seeds, and resurrection plants, both of which protect organisms against extreme desiccation in amorphous state (Sun and Leopold, 1997). Because of their simple structures and significant biological functions in nature, sucrose and trehalose are used as amorphous matrix in our study. They are both

non-reducing disaccharides, and their molecular structure and T_g have been showed in Table 1.

The non-radiative decay rates (k_{NR}) as a function of temperature for all 14 probes are plotted using an Arrhenius analysis in Fig. 19 and Fig. 20. They display a general phenomenal that probes have lower k_{NR} value in amorphous trehalose compared to probes in amorphous sucrose over the temperature range from 20 °C to 90 °C. Lower k_{NR} indicates probes staying in more rigid matrix with less molecular collision and quenching, the higher k_{NR} indicates probes staying in more mobile matrix with high possibility of molecular collision and quenching. Also, through these two figures, it depicts all these probes (except 5-bromotryptophan in Fig. 16) are very sensitive to the thermal dynamic change of the local environment in the both amorphous trehalose and sucrose matrix, and they provide very similar pictures to each other.

The insets in Fig. 19 are plots of phosphorescence activation energy as a function of temperature. Using equation 4, these activation energies were calculated based on corresponding Arrhenius analysis of $\log(k_{NR})$ as a function of $1/T$ above. And it depicts that activation energy in trehalose generally is lower than in sucrose at temperature from 20 °C to 80 °C for the same probe. The smaller phosphorescence activation energy in trehalose could be caused by localized and limited vibrational and/or rotational motions of matrix or water molecules that have lower intrinsic energy barriers (Ludescher et al., 2001). The energy barriers are influenced by many

factors, like free volume around probes, local structure and hydrogen-bonding interaction among matrix, water and probe. In all, amorphous trehalose is more rigid than sucrose over the temperature range from 20 °C -120 °C.

It is concluded that trehalose has a lower free volume in the glassy state as well as lower free volume expansion coefficient above T_g than sucrose due to a more tightly packed molecular structure (Sun and Davidson, 1998; Dranca et al., 2009;). Molecular packing in trehalose is more compact than in sucrose attributable to the nature of hydrogen bonding network present in trehalose. And sites with smaller free volume are more rigid and have lower activation energy (Ludescher et al., 2001). This is consistent with the results we have here.

About hydrogen bonding network, there are many hypothesis to illustrate the difference between sucrose and trehalose. First, trehalose has bisymmetric structure with two D-glucose rings, while sucrose is asymmetric composed with a glucose ring and a fructose ring. Phillips proposed that trehalose molecules at the glass state have a stable and flexible arrangement because of “tandem sandwich” structure that strongly bond pairs of glucose rings are alternated with weakly bound pairs (Phillip, 2006). However, due to ring asymmetry, glassy sucrose molecules are not possible to have this “sandwich” structure so that glassy sucrose is not packing better than glassy trehalose. In addition, it is reported that trehalose have stronger sugar-water interaction than sucrose (Longo et al., 2010). Sucrose has a more significant

competition between internal and external hydrogen bonds than in trehalose. In the other word, sucrose molecules have fewer external hydrogen bonds with the surrounding water molecules than trehalose at very low sugar/water ratio, so that sucrose molecules have lower effect on destructuring of the water network than trehalose (Ekdawi-Sever et al., 2001). The better sugar-water interaction ability of trehalose can constrain the water molecules so that molecule motions can be hindered to some extent.

Except hydrogen-bonding factor, it is also suggested that the different properties between trehalose and sucrose are related to the higher glass transition temperature of trehalose with respect to sucrose (Green and Andell, 1989). We have showed in Table 1 (Page 14) that amorphous trehalose has much higher T_g than amorphous sucrose. Namely, vibrational motions and limited rotational motions are still dominated in glassy trehalose when temperature reaches to 60 °C, while sucrose start to go through glassy state to melt state with the onset of translational motions. Therefore, the obvious difference of T_g is a also important reason why trehalose matrix is more rigid than sucrose.

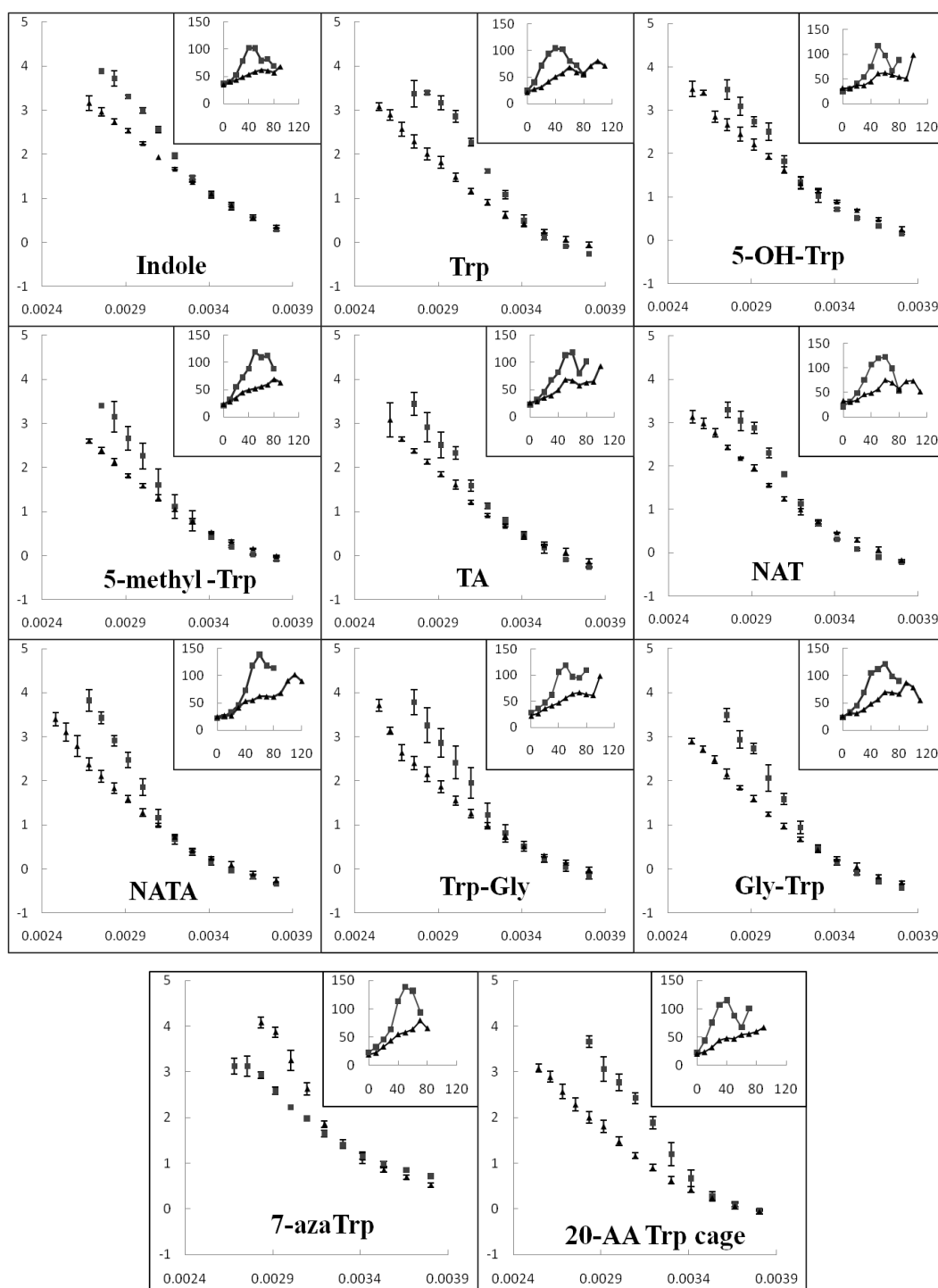


Fig. 19. $\log(k_{NR}/s^{-1})$ versus K/T for selected probes in amorphous sucrose and trehalose. Insets are the plots of E_a (kJ/mol) versus $T/^\circ C$ for corresponding probes in amorphous sucrose and trehalose. The applied probes are showed in the plots from left to right and up to down: Indole, Tryptophan, 5-methyl-tryptophan, Tryptophanamide (TA), N-Acetyltryptophanamide (NATA), Glycyltryptophan

(Gly-Trp), 7-aza-Trp, and 20-AA Trp-Cage protein. The data for all these probes in sucrose were measured every 10 °C from -10 °C to 80 °C ~90 °C. And the data for probes in trehalose were measured every 10 °C from -10 °C to 100 °C ~120 °C. The phosphorescence decay rates (k_{RP}) of 5-OH-Trp applied here is 0.293 s^{-1} and k_{RP} of 7-azaTrp is 3.22 s^{-1} (Sengupta et al., 2002). We assume that all probes else in this figure have same phosphorescence decay rates, 0.167 s^{-1} (Weinryb and Steiner, 1968). Solid grey square: probes in amorphous trehalose; Solid black triangle: probes in amorphous sucrose.

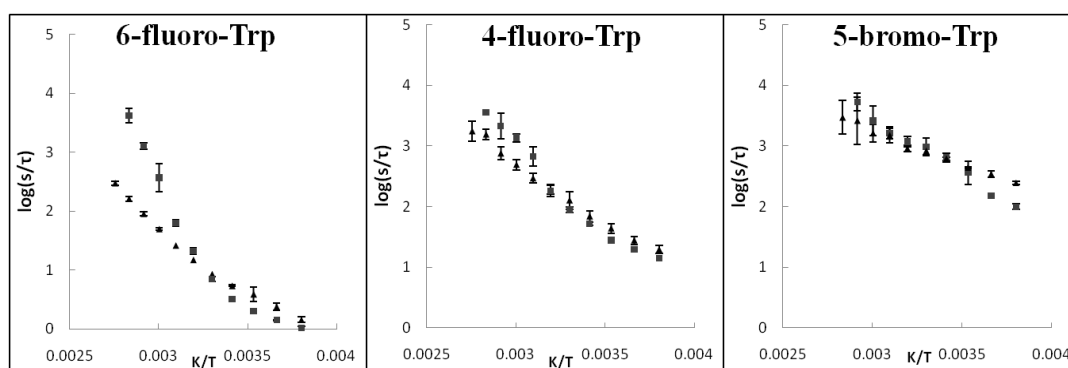


Fig. 20. $\log(s/\tau)$ versus K/T for selected probes in amorphous sucrose and trehalose.

Probes are showed from left to right and up to down: 6-fluoro-Trp, 4-fluoro-Trp, and 5-bromo-Trp. The data for these probes in sucrose were measured every 10 °C from -10 °C to 80 °C, in trehalose were measured every 10 °C from -10 °C to 90 °C. Solid grey square: probes in amorphous trehalose; Solid black triangle: probes in amorphous sucrose.

4. Comparison of Indole, Trp, TA, NAT, NATA, Trp-Gly and Gly-Trp

4.1. Indole and Trp

It was assumed that indole and tryptophan have same phosphorescence decay rate (k_{RP} , $1/6 \text{ s}^{-1}$) here. It is reported that the triplet lifetime of indole and NATA in aqueous environments at 20 °C was almost same (Fischer et al., 2001). However, there is no study about comparison of phosphorescence decay between indole and tryptophan (or tryptophan derivatives) in solid state. From Fig. 21, it shows that the non-radiative phosphorescence decay rates (k_{NR}) of indole is about 3~4-fold larger at -10 °C - 20 °C and about 1~2-fold larger at 30 °C - 50 °C than k_{NR} of tryptophan in sucrose matrix. Also, k_{NR} of indole is about 3~4-fold larger than k_{NR} of tryptophan in trehalose matrix at 0 °C -100 °C. Larger k_{NR} indicates less molecules motions, and lower k_{NR} stands for more mobile matrix. Generally, tryptophan is much more rigid than indole at the temperature below T_g in sucrose matrix as well as in trehalose matrix. Once temperature reaches to T_g and higher, the molecule mobility of tryptophan becomes similar to the one of indole in amorphous sucrose.

We suggest the above difference can be caused by stronger tryptophan-sugar interaction in glassy state. From structure of tryptophan, we know that tryptophan has indole group as a chromophore. And it not only has active hydrogen from amino in indole ring, but also has very active α -amino and carboxyl groups. And these two active groups in tryptophan can have hydrogen-bonding interaction with sugar and/or water in their local environment. Namely, tryptophan integrates more with

surrounding molecules (sugar and/or water) than indole. Our hypothesis is that tryptophan molecules are constrained to some extent because of the interaction with rigid sugar molecules at the glassy state so that tryptophan molecules are more rigid with less non-radiative decay than indole. However, when temperature reaches to T_g of sugar and higher, tryptophan and indole tend to have similar k_{NR} value in the Fig. 21. Sugar molecules at melt state are not rigid as molecules at glassy state anymore. The sugar molecules become very mobile with translational motions, which decrease the hydrogen-bonding interaction with tryptophan as well as have fewer effects on “fixing” tryptophan molecules. And this can be possible reason that k_{NR} value of tryptophan is similar to one of indole in sucrose matrix at the temperature above T_g .

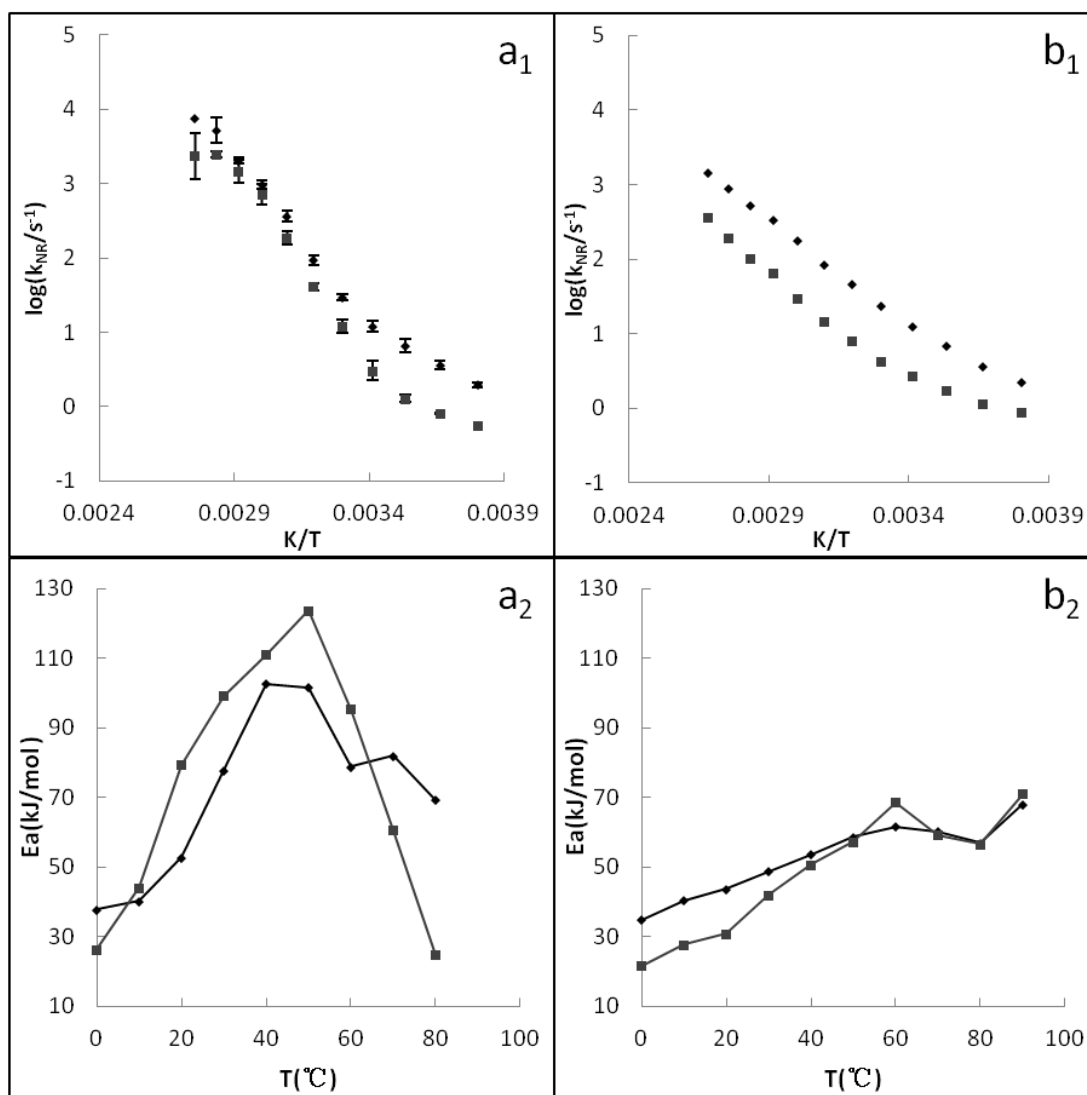


Fig. 21. Comparison of non-radiative phosphorescence decay for indole and tryptophan. Fig. 21a₁ and Fig. 21b₁ show Arrhenius analysis of non-radiative phosphorescence rate (k_{NR}/s^{-1}) respectively in the sucrose (Fig. 21a₁) and in trehalose amorphous matrix (Fig. 21b₁). And Fig. 21a₂ and Fig. 21b₂ are plots of phosphorescence activation energy as a function of temperature based on Fig. 21a₁ and Fig. 21b₁. The data for indole and tryptophan in sucrose were measured every 10 °C from -10 °C to 90 °C, and in trehalose were measured every 10 °C from -10 °C to 100 °C. Solid grey square: tryptophan; Solid black rhombus: indole.

4.2. Trp, Gly-Trp and Trp-Gly

From Fig. 22, it was clear that Trp, Trp-Gly, and Gly-Trp all showed strong sensitivity to the molecular motion of local environment. The phosphorescence activation energy as a function of temperature is very close for these three probes in sucrose matrix, and is almost same when these three probes in trehalose matrix. The similar phosphorescence activation energy at each specific temperature suggests that no matter Trp bind with Gly at N-side or C-side, the additional Gly binding with Trp does not influence on probes response to the thermodynamics of surrounding matrix.

k_{NR} of Trp-Gly and Trp are very close both in sucrose matrix and trehalose matrix. However, the k_{NR} of Trp-Gly is constantly about one fold larger than k_{NR} of Gly-Trp in sucrose matrix at -10 °C to 90 °C as well as in trehalose matrix at -10 °C to 110 °C. It was reported that Trp-Gly has an intra-ring when they are at the most stable state, while Gly-Trp does not have by computational calculation (Hünig and K. Kleinermanns, 2004; Valdes et al., 2006). The free carboxylic group on the c-terminus of Trp-Gly can have a strong hydrogen bond with the carbonyl group of the peptide bond (Fig. 23 and Fig. 24). Through computational model, this intramolecular hydrogen-bonding interaction induce Trp-Gly to have proton transfer once molecular from singlet excited state to the ground state. It was said that a conical intersections of the charge-transfer state with the electronic ground state cause the electronic excitation energy convert into vibrational energy, which increase excited-state deactivation of Trp-Gly and may is the reason that this structure (Fig.

24) cannot be detected in REMPI spectrum (Shemesh et. al., 2009). Shemesh also found the excited-state deactivation because of intermolecular hydrogen bonds in Gly-Phe-Ala tripeptide (Shemesh et. al., 2008). Even though Shemesh study is based on the model for trp-gly from singlet excited state to ground state, we suggest that the proton transfer in Trp-Gly may also be the reason of the high phosphorescence non-radiative rate. The constant larger k_{NR} of Trp-Gly than Gly-Trp suggests that proton transfer of Trp-Gly is a temperature independent quenching effect, which increases the k_{NR} of Trp-Gly.

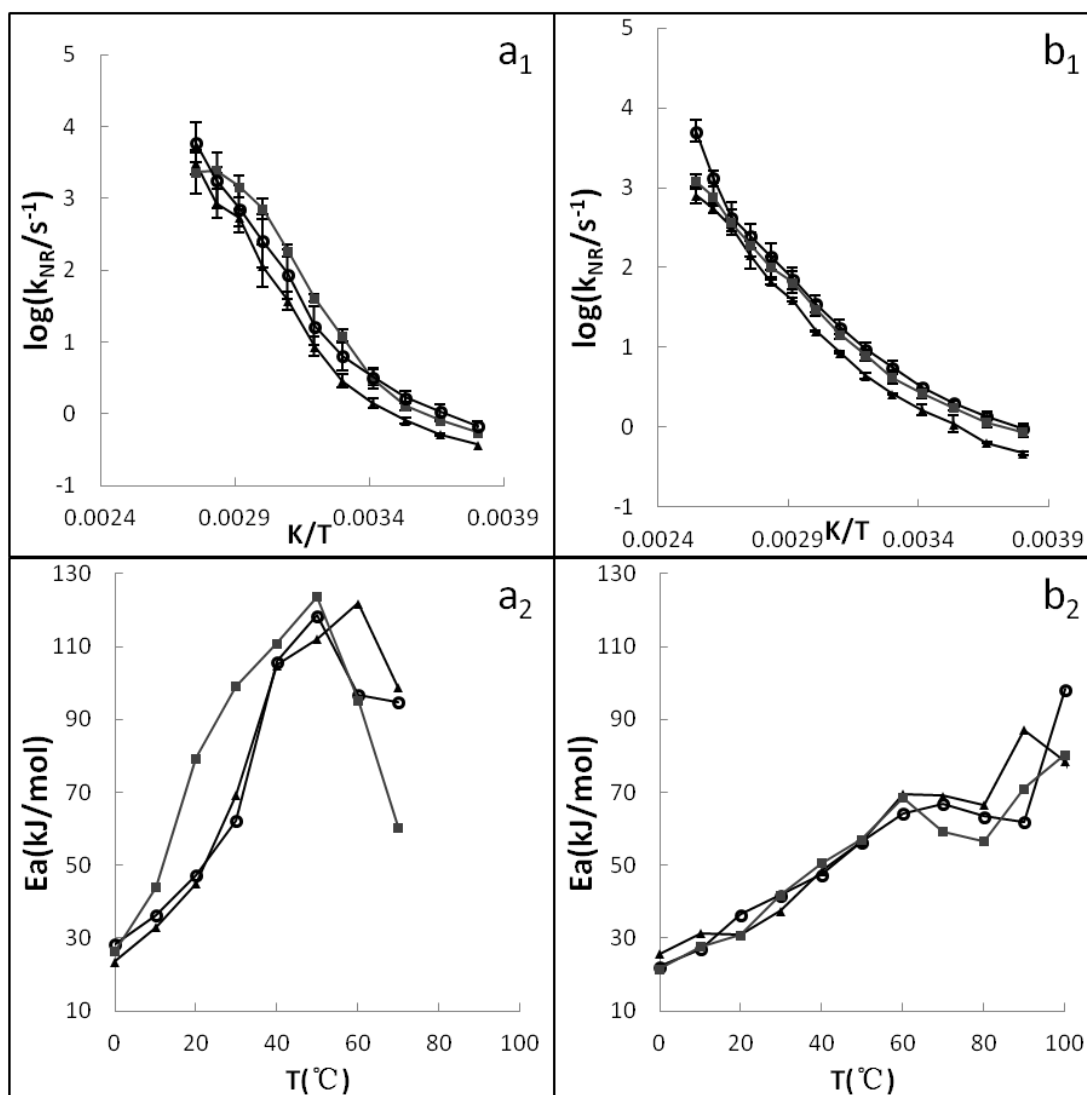


Fig. 22. Non-radiative phosphorescence decay for probes (Trp, Trp-Gly, and Gly-Trp). Arrhenius analysis of k_{NR} (s^{-1}) as a function of temperature has been showed for these three probes in sucrose matrix (Fig. 22a₁) and in trehalose matrix (Fig. 22b₁). And Fig. 22a₂ and Fig. 22b₂ are plots of phosphorescence activation energy as a function of temperature based on Fig. 22a₁ and Fig. 22b₁ correspondingly. The data in sucrose were measured every 10 °C from -10 °C to 90 °C, and in trehalose were measured every 10 °C from -10 °C to 120 °C. Solid grey square: tryptophan; Open circle: Trp-Gly; Solid black triangle: Gly-Trp.

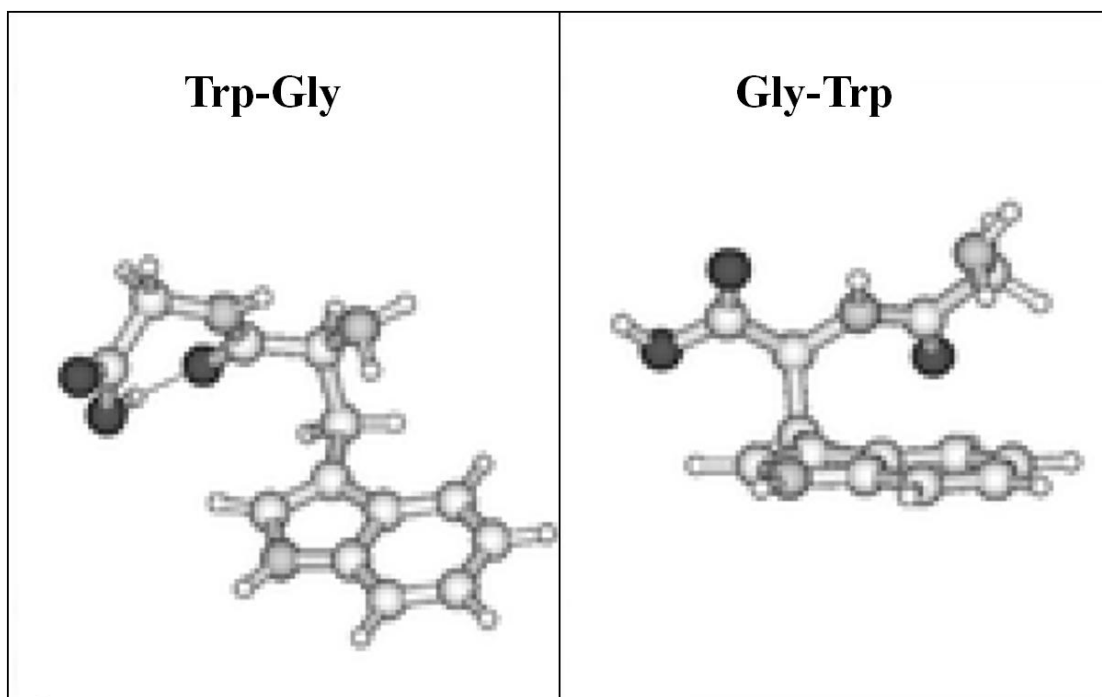


Fig. 23. The lowest energy level structure for Trp-Gly and Gly-Trp (Hünig and Kleinermanns, 2004)

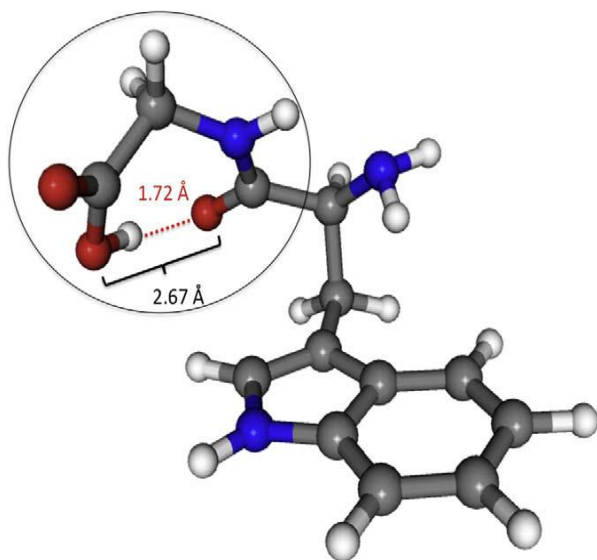


Fig. 24. The most stable conformer of Trp-Gly. The ellipse encircles a hydrogen-bond motif in Trp-Gly (Shemesh et. al., 2009; Valdes et al., 2006).

4.3. Gly-Trp vs. NAT and Trp-Gly vs. TA

It is known that TA and Trp-Gly both have structure that additional groups ($-\text{NH}_2$ for TA; $-\text{NH}-\text{CH}_2-\text{COOH}$ for Trp-Gly) are bound at Trp-COOH side; NAT and Gly-Trp both have structure that additional groups ($-\text{CO}-\text{CH}_3$ for NAT; $-\text{CO}-\text{CH}_2-\text{NH}_2$ for Gly-Trp) are bound at Trp- NH_2 side. Therefore, we compare TA and Trp-Gly as well as NAT and Gly-Trp here. From Fig. 25, it shows that the non-radiative phosphorescence decay rates (k_{NR}) of TA and Trp-Gly are close both in sucrose and trehalose, while k_{NR} of NAT and Gly-Trp have small temperature independent difference in sucrose and trehalose. In all, TA, NAT and Trp-Gly show very close shape curves in the above Arrhenius analysis, and Gly-Trp shows similar curves except lower k_{NR} compared with the above probes. Hence, these four probes with different structure do not influence Trp phosphorescence very much, and they all still very sensitive to the surrounding matrix.

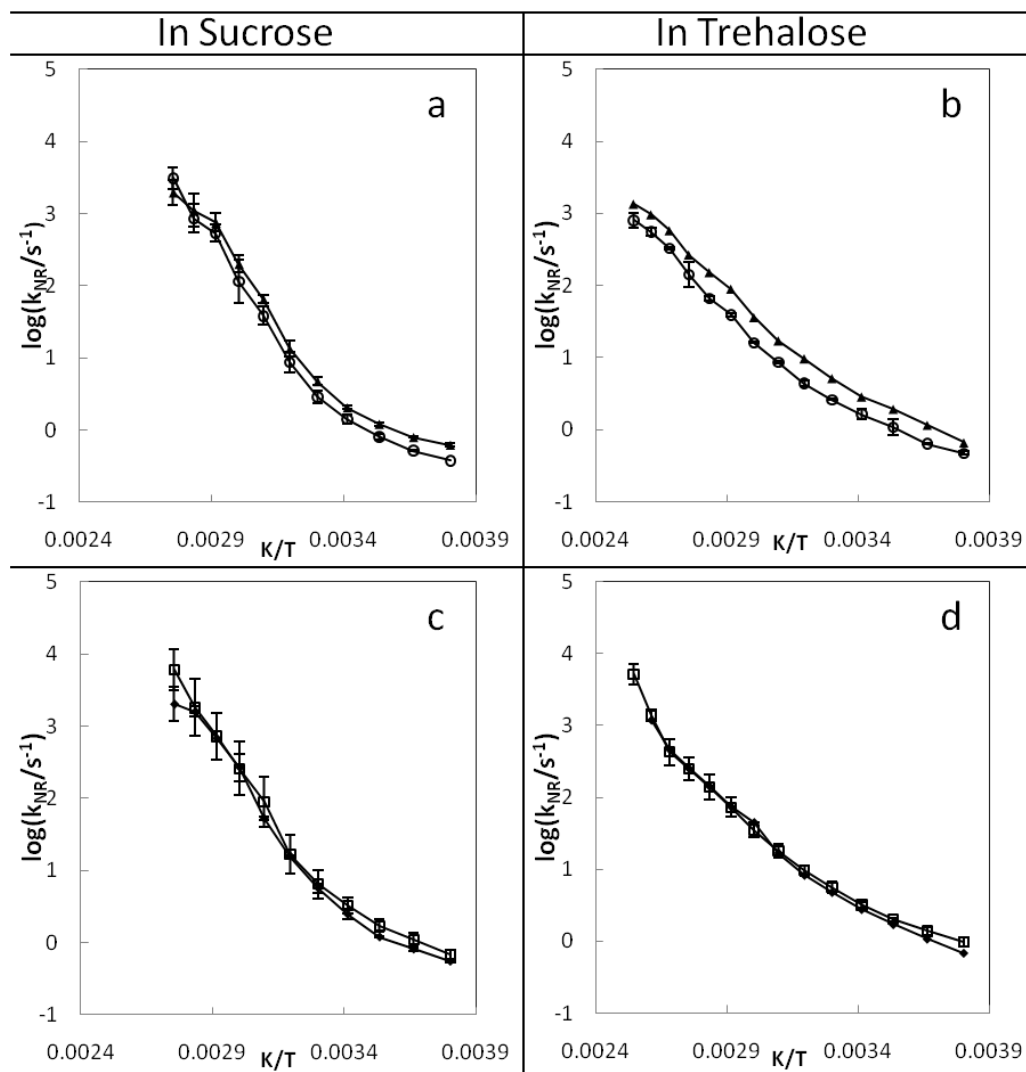


Fig. 25. Non-radiative phosphorescence decay for probes (NAT, Gly-Trp, TA, Trp-Gly). Arrhenius analysis of k_{NR} (s^{-1}) as a function of temperature has been showed for NAT and Gly-Trp in sucrose matrix (Fig. 25a) and in trehalose matrix (Fig. 25b), for TA and Trp-Gly in sucrose matrix (Fig. 25c) and in trehalose matrix (Fig. 25d). The data for these probes in sucrose were measured every $10^{\circ}C$ from $-10^{\circ}C$ to $90^{\circ}C$, and in trehalose were measured every $10^{\circ}C$ from $-10^{\circ}C$ to $120^{\circ}C$. Solid black triangle: NAT; Open circle: Gly-Trp; Solid black rhombus: TA; Open Square: Trp-Gly.

4.4. Trp, TA, NAT and NATA

In the Fig. 26, it have showed that Trp, TA, and NAT have close Arrhenius analysis both in sucrose and trehalose matrix, while NATA have lower k_{NR} compared to the above three. NATA has a structure with both additional $-\text{CO}-\text{CH}_3$ (NAT has) on amino side of tryptophan and $-\text{NH}_2$ (TA has) on carboxyl side of tryptophan. In the Fig.26, it depicts no big difference of non-radiative decay among TA, NAT and tryptophan in glassy trehalose over the temperature range from $-10\text{ }^{\circ}\text{C}$ to $120\text{ }^{\circ}\text{C}$, while tryptophan shows a little different k_{NR} trend from TA and NAT in the sucrose matrix at the temperature from $20\text{ }^{\circ}\text{C}$ - $80\text{ }^{\circ}\text{C}$. NATA has the lowest k_{NR} value both in amorphous sucrose and trehalose, but neither TA or NAT can show similar low non-radiative decay to NATA. There would be a synergetic effect by additional $-\text{CO}-\text{CH}_3$ and $-\text{NH}_2$ groups to make NATA integrate more with surround sugar matrix so that NATA has lower k_{NR} compared to Trp, TA and NAT. However, we have not known the mechanism in phosphorescence decay of NATA in amorphous sugar yet.

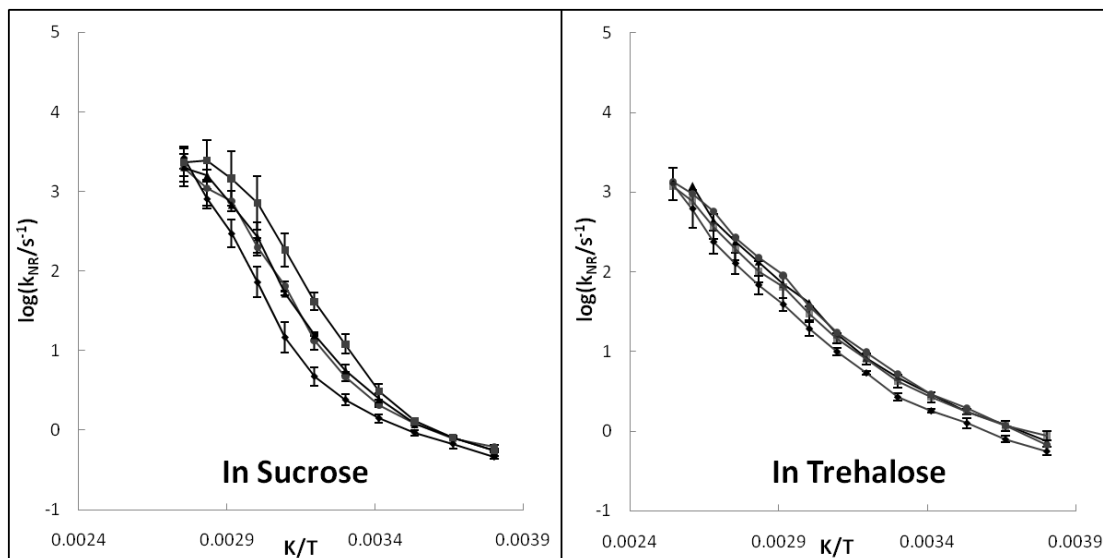


Fig. 26. Arrhenius analysis of k_{NR} (s^{-1}) as a function of temperature for probes (TA, NAT, NATA, Trp) in sucrose matrix and in trehalose matrix. The data for these probes in sucrose were measured every 10 °C from -10 °C to 90 °C, and in trehalose were measured every 10 °C from -10 °C to 120 °C. Solid black triangle: TA; Solid grey circle: NAT; Solid black rhombus: NATA; Solid grey square: Trp.

5. Comparison of tryptophan, 5-hydroxytryptophan and 5-methyltryptophan

Here, we assume that the phosphorescence decay rate k_{RP} of 5-methyl-Trp is 0.167 s^{-1} . And phosphorescence lifetime at 77 K of 5-OH-Trp, 3.41 s, is applied in our study (Sengupta et. al., 2001). The phosphorescence non-radiative decay rates of 5-methyltryptophan are very similar to tryptophan both in sucrose and in trehalose (Fig.27). However, the additional 5-hydroxyl in the indole ring part of Trp causes an obvious larger k_{NR} in the rigid sugar glass (Fig.27). The additional methyl group does not like hydroxyl group, which can integrate with surrounding matrix by available hydrogen bonding. Therefore, we suggest that a hydrogen-bonding interaction between 5-OH-Trp and surrounding matrix increases non-radiative phosphorescence rate in the glassy sugar matrix. Since k_{NR} value of 5-OH-Trp is close to k_{NR} value of 5-methyl-Trp at 40°C - 90°C in sucrose matrix, the effect of hydrogen-bonding interaction probably decrease or disappear once the temperature reaches to T_g and above. But, the k_{NR} value of tryptophan was a little higher than 5-methyl-Trp and 5-OH-Trp at 40°C ~ 80°C in amorphous sucrose. The activation energy of tryptophan was also larger than the other two in sucrose over the temperature range from 0°C to 50°C . However, it is not clear that why tryptophan shows different k_{NR} from the other probes in sucrose matrix now.

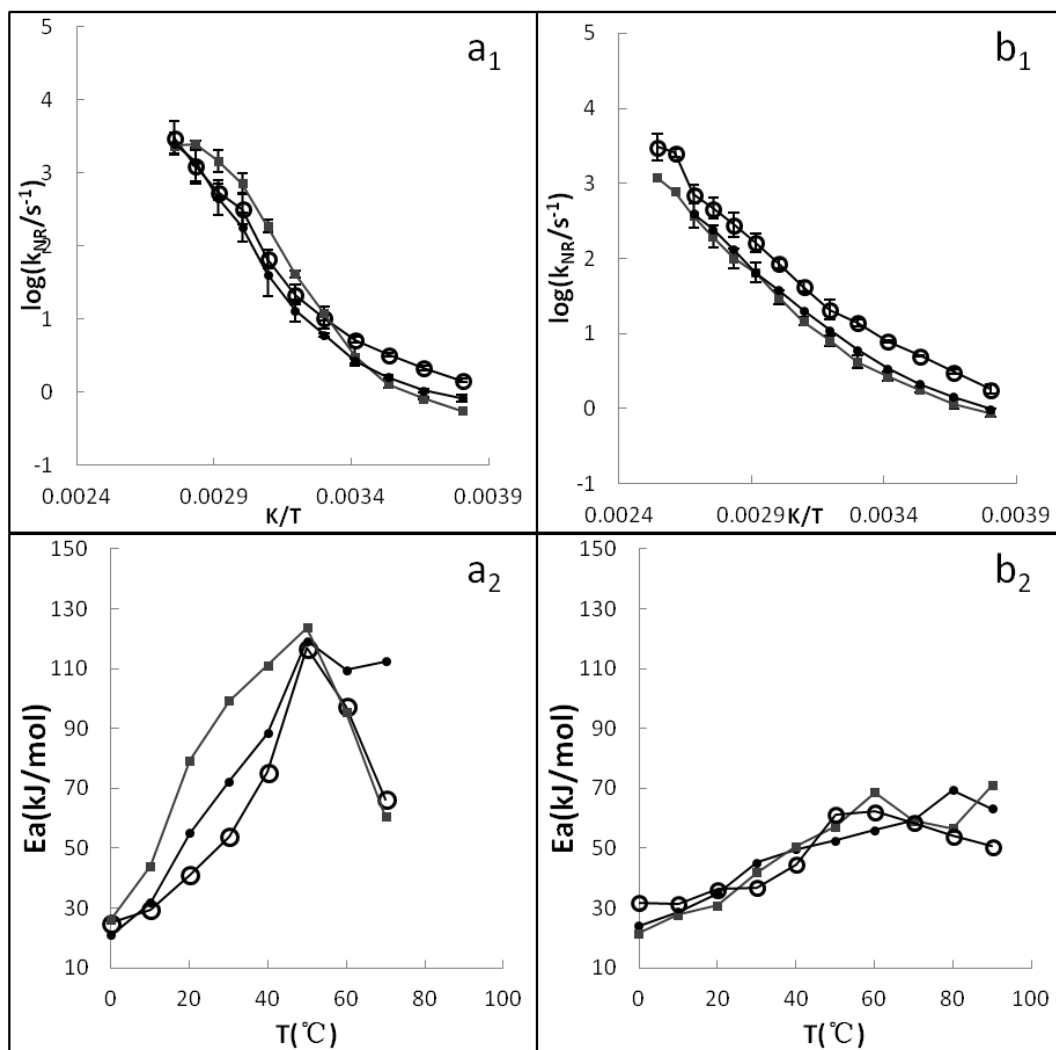


Fig. 27. Non-radiative phosphorescence decay for probes (tryptophan, 5-hydroxyl-tryptophan, and 5-methyl-tryptophan). Arrhenius analysis of k_{NR} (s⁻¹) as a function of temperature has been showed for these three probes in sucrose matrix (Fig. 27a₁) and in trehalose matrix (Fig. 27b₁). And Fig. 27a₂ and Fig. 27b₂ are plots of phosphorescence activation energy as a function of temperature based on Fig. 27a₁ and Fig. 27b₁ correspondingly. The data in sucrose were measured every 10 °C from -10 °C to 90 °C, and in trehalose were measured every 10 °C from -10 °C to 100~120 °C. Solid grey square: tryptophan; Solid black circle: 5-methyl-tryptophan; open circle: 5-hydroxyl-tryptophan.

6. Comparison of tryptophan and 4-fluorotryptophan, 6-fluorotryptophan, and 5-bromotryptophan

From Fig. 28, it shows that 4-fluorotryptophan has significant lower τ than tryptophan. 4-fluorotryptophan actually has very strong fluorescence and phosphorescence at low temperature (77 K) (Hott and Borkman, 1989). However, 4-fluorotryptophan is much more photolabile than tryptophan. It was reported that 4-fluorotryptophan has a 7 times larger photolysis quantum yield than tryptophan at 25 °C (Hott and Borkman, 1989). Therefore, It is suggested that a fast reaction pathway from the excited triplet state of 4-fluorotryptophan may exist, which causing more photolabile than tryptophan and resulting in phosphorescence quenching.

Secondly, 6-fluorotryptophan has similar phosphorescence lifetime to tryptophan both in sucrose and trehalose matrix at the certain range of temperature (Fig. 28). It was reported that the quenching efficiency for the triplet state of tryptophan is 23-fold smaller than 4-fluorotryptophan, while only 2-times smaller than 6-fluorotryptophan at 20 °C (McCaul and Ludescher, 1999). Therefore, compared to 4-fluorotryptophan, 6-fluorotryptophan has similar photophysical properties to that of tryptophan

At last, 5-bromotryptophan has the lowest phosphorescence lifetime both in sucrose and trehalose matrix because of the presence of a heavy atom, bromine. Bromine atom with standard atomic weight, 79.90, is much heavier than fluorine atom with

standard atomic weight, 19.00. Therefore, 5-Br-Trp has more obvious heavy atom effect than 4-F-Trp and 6-F-Trp. Heavy atom effect is used to illustrate the influence of “heavy atom” substitution on spin-forbidden transitions, including S_1 to T_1 , T_1 to S_1 , and T_1 to S_1 . Through enhancing the spin-orbit coupling, heavy atom effect can influence on phosphorescence radiative/non-radiative decay rate as well as intersystem crossing rate. It was suggested that the presence of fluorine atom substitution in 4-F-Trp and 6-F-Trp only modulates the non-radiative rate constant for deexcitation of the triplet state and does not modulate either k_{ISC} or k_{RP} . But, for 5-Br-trp, the bromine atom substitution not only increases the intersystem crossing rate, but also the intrinsic phosphorescence decay rate (McCaul and Ludescher, 1999).

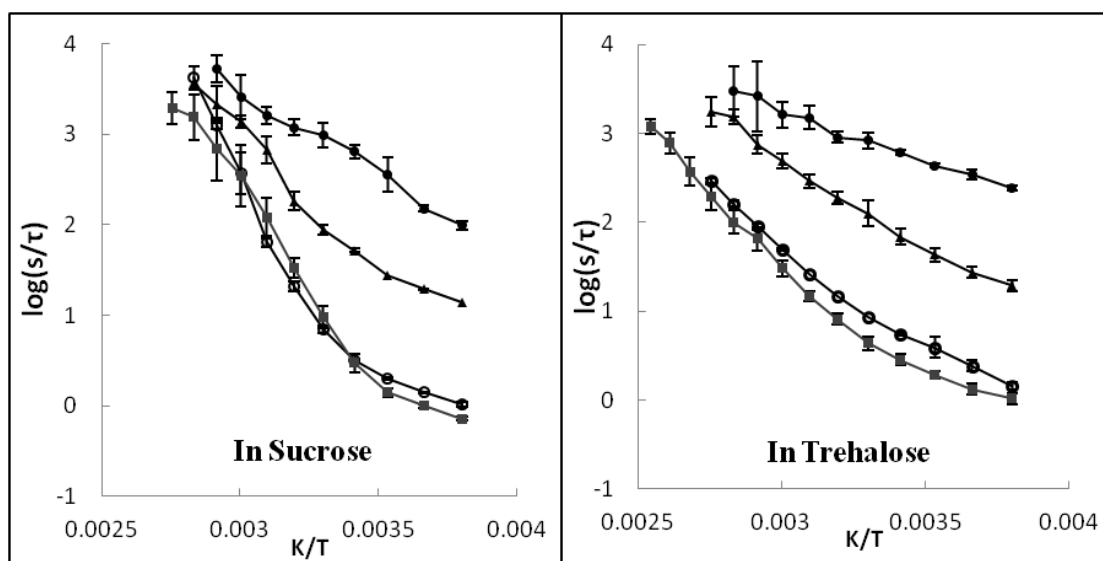


Fig. 28. Phosphorescence lifetime decay by Arrhenius analysis for probes (tryptophan, 5-bromotryptophan, 4-fluorotryptophan and 6-fluorotryptophan) both in amorphous sucrose matrix and trehalose matrix. The data for all these probes in sucrose were measured every 10 °C from -10 °C to 70 °C ~90 °C. And the data in trehalose were measured every 10 °C from -10 °C to 80 °C ~120 °C. Solid grey square: tryptophan; Solid black circle: 5-bromotryptophan; open circle: 4-fluorotryptophan; solid black triangle: 6-fluoro-tryptophan.

7. Comparison of tryptophan and 7-azatryptophan

Two existing phosphorescence lifetimes of 7-azatryptophan in ethanol at 77 K were reported, 3.22 s and 1.02 s (Sengupta et. al., 2001). A long phosphorescence lifetime of 7-azaindole was also reported by Ilich, 3.78s (Ilich, 1995). And we applied the phosphorescence lifetime (3.22 s) to 7-azatryptophan in sucrose and trehalose here.

The k_{NR} value of 7-azatryptophan is always about 6~8-fold larger than one of tryptophan at -10 °C to 90 °C in trehalose matrix. In addition, k_{NR} of 7-azatryptophan is about 6-fold larger at -10 °C to 20 °C and about 2-fold larger at 30 °C to 60 °C than k_{NR} of tryptophan in sucrose matrix (Fig. 29). Moreover, phosphorescence activation energies of these two probes are a little difference in sucrose matrix, while they are very close in trehalose matrix.

The substitution of N for C in pyridine group of tryptophan can cause two hydrogen bonds in 7-Aza-Trp by donating the pyrrole proton and accepting a proton at the pyridine nitrogen. And this hydrogen-bonding interaction can lead 7-azatryptophan to associate with the surrounding sugar and/or water molecule, or 7-azatryptophan can associate with itself to form dimer (Ingham and El-Bayoumi, 1974; Matsui et al., 1989). It was important to note that no dimer and no tautomer of 7-azaindole have been detected in a rigid solvent matrix (Taylor et al., 1969; Ilich, 1994). Since rigid condition of amorphous sugar matrix in our study, we suggest that 7-azatryptophan monomer is dominant molecule type in sugar glass, which can have hydrogen-bonding interaction with surrounding sugar and/or water molecules.

Ilich has explained that phosphorescence emission loss of 7-azaindole could be caused by transition from $T_1\{\pi^*\}$ to $S_0\{n\}$ in glycerol/water glass (Ilich, 1994). Through computational calculation, Ilich suggested that there is an additional interleaved $T(\pi^*, n)$ between the highest triplet excited state level and the lowest triplet excited state level. This additional state was also approved by the other calculation method (Serrano-Andrés and Borin, 2000). Because of the strong hydrogen-bonding interaction of 7-azaindole with sugar and/or water, 7-azaindole has the delocalized non-bonding orbital compared to indole. This delocalization not only lowers the energy gap from $T_1\{\pi^*\}$ to $S_0\{n\}$, but also increases the phosphorescence non-radiative rate.

Since the additional 5-hydroxyl group in 5-OH-Trp also have potential hydrogen-bonding interaction with surrounding sugar and/or water, this mechanism could be applied in 5-hydroxytryptophan. 5-hydroxytryptophan can have delocalized non-bonding orbital and lower energy gap between the ground non-bonding state and the triplet excited state, which increase the non-radiative efficiency. In our result, it shows 5-hydroxytryptophan also have larger k_{NR} than tryptophan at rigid sugar glassy state (Fig. 27). This is consistent with the suggestion above.

In the rigid glassy state, the association between 7-azatryptophan and surrounding sugar/water molecules is stable so that k_{NR} of 7-azatryptophan shows stable different from one of tryptophan on sucrose matrix at -10 °C -20 °C and in trehalose at -10 °C

-90 °C (Fig. 29). Moreover, this hydrogen-bonding interaction may become weak and the quenching effect by this association may decrease when temperature arrives to T_g and above because of increasing molecule motions. This could be a reason why tryptophan and 7-azatryptophan have smaller different k_{NR} at 30 °C -60 °C in sucrose matrix.

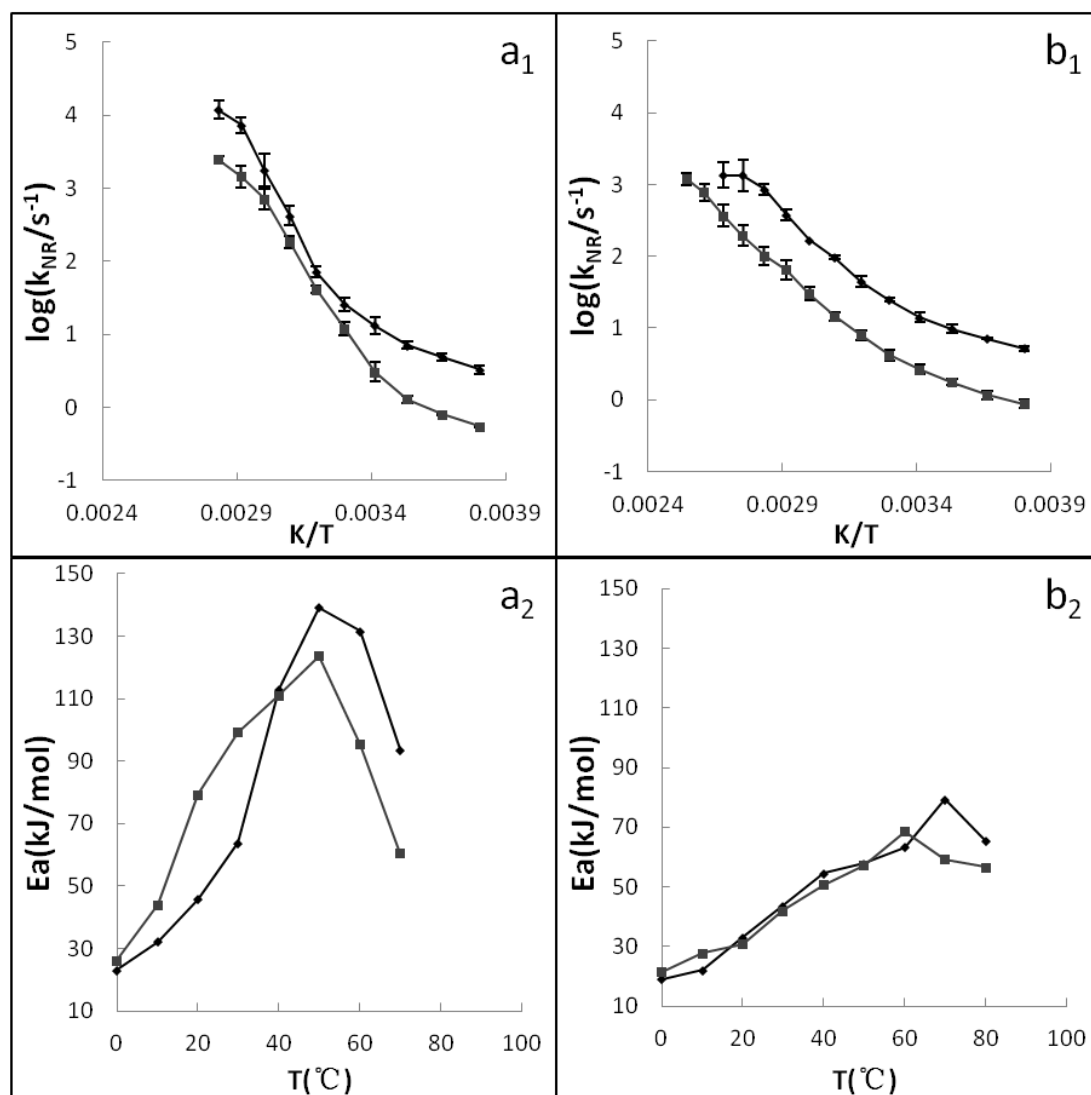


Fig.29. Non-radiative phosphorescence decay between tryptophan and 7-azatryptophan. $\log(k_{NR}/s^{-1})$ vs. K/T for tryptophan and 7-azatryptophan in amorphous sucrose matrix (Fig. 29a₁) and in amorphous trehalose matrix (Fig. 29b₁). Fig. 29a₂ and Fig. 29b₂ are plots of phosphorescence activation energy as a function of temperature based on Fig. 29a₁ and Fig. 29b₁ correspondingly. The data for indole and tryptophan in sucrose were measured every 10 °C from -10 °C to 80 °C, and in trehalose were measured every 10 °C from -10 °C to 100 °C ~120 °C. Solid grey square: tryptophan; Solid black rhombus: 7-azatryptophan.

8. Comparison of tryptophan, Trp-Cage protein and HSA

The k_{NR} values between Trp-cage protein and Trp are very close both in sucrose and trehalose matrix (Fig.30). However, k_{NR} of HSA is about 4~5-fold larger than k_{NR} of Trp in trehalose matrix at -10 °C ~90 °C. Moreover, k_{NR} of HSA is about 3~4 times larger than k_{NR} of Trp in sucrose matrix at -10 °C ~20 °C, and k_{NR} of HSA shows less temperature dependence than tryptophan so that k_{NR} of HSA becomes smaller than k_{NR} of tryptophan as temperature increase to 40 °C and above. In addition, the phosphorescence activation energies of Trp, Trp-cage protein and HSA display similar in trehalose matrix at the above temperature range (Fig. 30b₂), which mean the molecule mobility of the local environment with these different probes is similar in amorphous trehalose.

Trp-Cage protein is a synthetic 20-residue polypeptide with sequence as NLYIQ WLKDG GPSSG RPPPS. It can fold spontaneously and cooperatively to a “Trp-cage”. Three proline residues (Pro-12, Pro-18, Pro-19) and a glycine (Gly-11) in this Trp-cage can interact together to form a compact hydrophobic core, which pack the Trp-6 side chain and Tyr-3 side chain inside and shield them from surrounding environment (Neidigh et al., 2002; Ahmed et al., 2005; Qiu et al., 2002). And the structure of Trp-cage protein is shown in Fig. 31 at the lowest energy level. In addition, it was showed that 90%-95% of this trp-cage exists in the native conformation at 4 °C in solution (Neidigh et al., 2002; Streicher and Makhatadze, 2007). HSA is a 585-residue macromolecular protein with single one tryptophan

embedded inside.

It was showed that only four amino acids, Phe (F), Tyr (Y), Cys (C), and His (H), in a sequence are able to quench Trp phosphorescence at a detectable rate, in the order Cys>> His+>Tyr>>Phe~His, when these four amino acids can contact with tryptophan residue under the distance range of interaction and they can have desirable space for molecular orientation with tryptophan(Gonnelli and Strambini, 2005; Gonnelli and Strambini, 1995). In Trp-cage sequence, we know that only one Tyr existing, which was also packed in the hydrophobic core. It can be suggested that there is no strong intramolecular quenching in Trp-cage, and quenching effect from Tyr-3 is very small and not observable, which may is because of the tightly packed structure of Trp-cage protein with sever restriction orientation. And in HSA sequence, it was reported that there are 35 Cys, 18 Tyr, 31 Phe, and 16 His (Meloun et al., 1975). However, it was not clear whether those amino acids in HSA have a strong influence on their larger k_{NR} .

Moreover, Trp-cage protein is a small molecule with only 20 residues so that there are not many water and sugar molecules directly interacting with it compared to HSA. More molecules surrounding HSA interact with protein could increase the entropic search of probe, which could increase the efficiency of non-radiative decay. Furthermore, we mentioned before that tryptophan in Trp-cage protein is packed tightly by the interaction among three proline residue and a glycine in the sequence.

Therefore, the probably reason for HSA with higher k_{NR} could also be the larger free volume at tryptophan side chain, compared to Trp-cage protein.

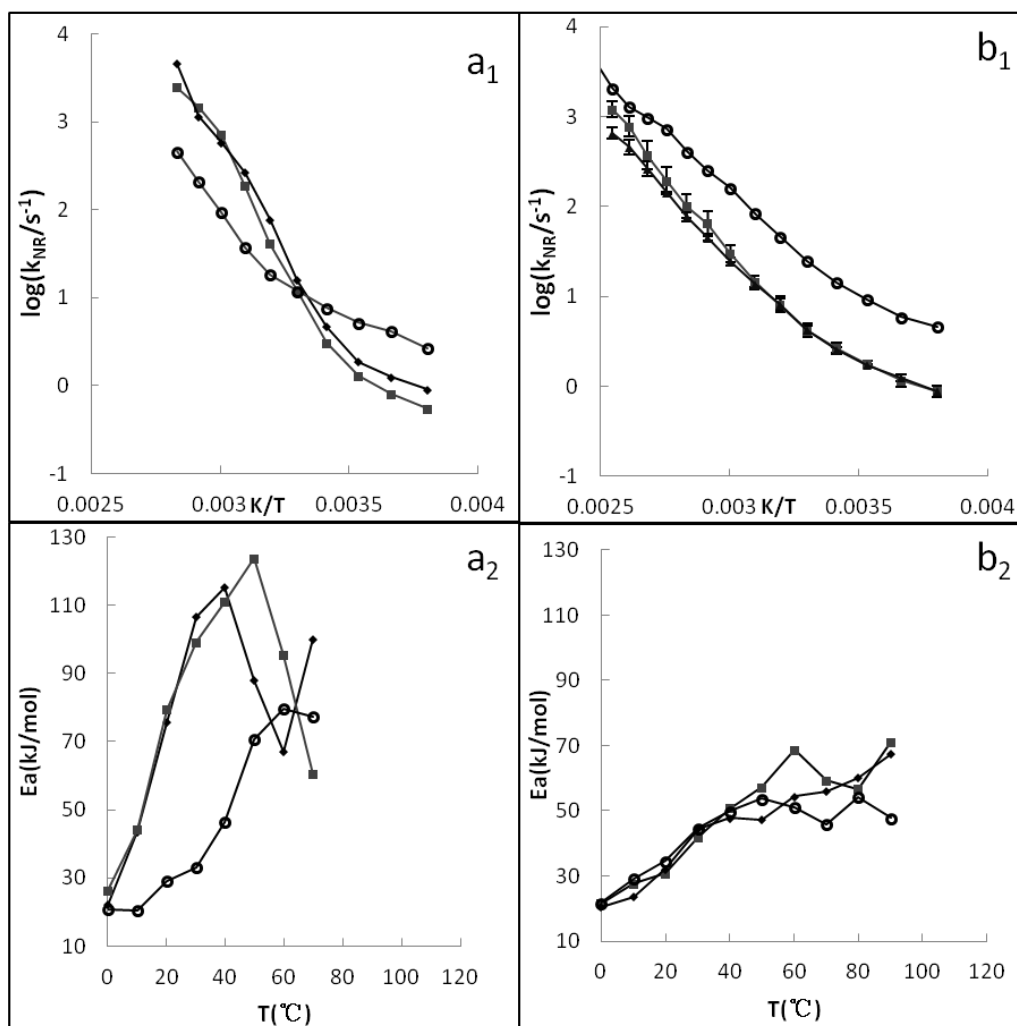


Fig. 30. Non-radiative phosphorescence lifetime decay of tryptophan, Trp-Cage protein and human serum albumin (HSA). Arrhenius analysis of non-radiative phosphorescence decay rate as a function of temperature for these three probes in sucrose matrix (Fig. 30a₁) and in trehalose matrix (Fig. 30b₁). Fig. 30a₂ and Fig. 30b₂ are plots of phosphorescence activation energy of these probes as a function of temperature based on the data in Fig. 30a₁ and Fig. 30b₁ correspondingly. The data for indole and tryptophan in sucrose were measured every 10 °C from -10 °C to 80 °C, and in trehalose were measured every 10 °C from -10 °C to 120 °C. Solid grey square: tryptophan; Solid black triangle: Trp-Cage protein; Solid black circle: HSA. (The HSA data is from my labmate Andrew Draganksi in Dr. Ludescher's lab.)

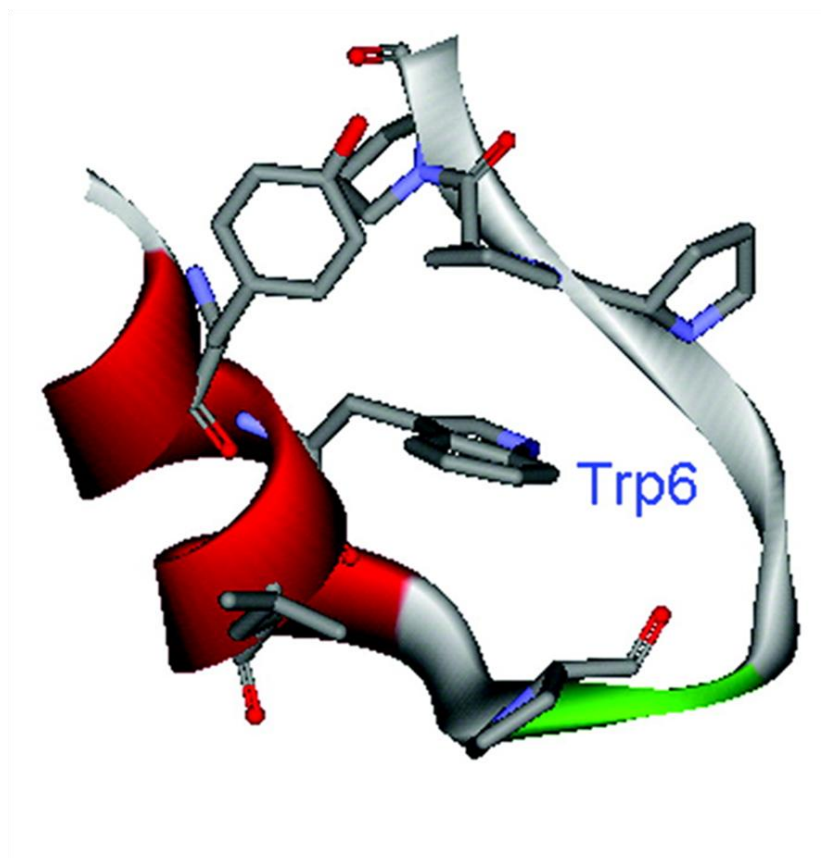


Fig. 31. Lowest level energy structure of Trp-Cage protein. The key hydrophobic residues packing against the central Trp-6 residue (Tyr-3, Trp-6, Leu-7, Pro-12, Pro-17, Pro-18, and Pro-19) are shown in sticks and all other residues are shown in ribbons. (Zhou, 2003)

CONCLUSION

It has been reported that factors, like conformation, molecular size, molecular packing, hydrogen bonded interactions and local structure, influence on the physical properties of amorphous carbohydrate matrixes (Limbach and Ubbink, 2008; Townrow et al., 2007; You and Ludescher, 2010). In our study, it shows that trehalose is more rigid than sucrose in amorphous solid state. And the possible factors causing these two disaccharides differ are their different glass transition temperatures as well as their various hydrogen-bonding interaction which may cause smaller free volume and more constrained water molecules in amorphous trehalose than sucrose .

For chromophore exposure to matrix, there are several factors which impact on phosphorescence decay. First, probes like 5-OH-Trp and 7-azatryptophan can have intermolecular hydrogen-bonding with surrounding sugar matrix and/or water, and this interaction increases the efficient of non-radiative decay rate at the triplet state. Second, Trp-Gly has intramolecular hydrogen-bonding by the interaction of the free carboxylic group on the c-terminus and the carbonyl group of the peptide bond at its lowest energy level. This intramolecular hydrogen-bonding can cause proton transfer when molecular go back to ground state from excited state. It was suggested that this proton transfer is the reason of increasing non-radiative decay rate for probes from excited singlet state to the ground state. In our study, it depicts that Trp-Gly has the larger k_{NR} than Gly-Trp. Therefore, we suggest that this proton transfer may also exist at the triplet state and is the reason for the larger k_{NR} of Trp-Gly. Compared these two

possible hydrogen-bonding effects, the intra one seems temperature independent, while the inter effect decreases when sugar matrix from glassy state to melt state at high temperature. Moreover, the heavy atom effect by additional fluorine and bromine (bound at indole ring group of tryptophan) is very obvious in our study. The binding site of heavy atom at indole ring would influence on this effect. 4-F-Trp is much more quenched with respect to 6-F-Trp. Also, the heavier weight of atom, Bromine, has more effect on inducing non-radiative decay at the triplet state. Furthermore, there would be a synergetic effect by additional two groups, $-\text{CO}-\text{CH}_3$ at amino side and $-\text{NH}_2$ at carboxyl acid side on tryptophan, to make NATA as the most rigid probe with lowest k_{NR} value both in amorphous sucrose and trehalose compared to Trp, TA and NAT, while this synergetic effect is not clear yet.

For chromophore not exposure to the matrix (Trp-cage protein and HSA), Trp-cage protein has similar phosphorescence property to tryptophan while HSA has a large quenching effect at glassy sugar compared to Trp. Intramolecular quenching by some amino acids, free volume of trp-site at local environment, size of protein intersurface where protein directly interact with surrounding matrix, and protein entropic search are possible factors that have impacts on non-radiative phosphorescence decay rate of protein with Trp packed inside. Trp-cage, since it is a miniprotein with only 20 residues and only one Tyr in the sequence as well as trp is packed tightly, has similar non-radiative phosphorescence decay to Trp. However, HSA is a 585-residues protein with a large molecular surface so that more surrounding sugar matrix and

water can interact with it. The lots of molecules around interacting with HSA would increase the entropic search of HSA and then induce more energy at the excited state goes to non-radiative decay at the triplet state.

In summary, the present investigation examined that many factors existing from probes itself and/or matrix can affect the Tryptophan phosphorescence. However, more phosphorescence data about different characteristic small molecules still is required to have a better understanding about what phosphorescent probes tells us about matrix properties in glass forming solvents.

REFERENCES

- Ahmed Z., Beta I. A., Mikhonin A. V. and Asher S. A. 2005. UV-Resonance raman thermal unfolding study of Trp-Cage shows that it is not a simple two-state miniprotein. *J. Am. Chem. Soc.* 127: 10943-10950.
- Bhandari B.R. and Howes T., 1999. Implication of glass transition for the drying and stability of dried foods. *J. Food Eng.* 49: 71-79.
- Crowe J. H., Carpenter J. F., Crowe L. M. 1998. The role of verification in anhydrobiosis. *Annu. Rev. Physiol.* 60: 73-103.
- Demchenko A.P., Ultraviolet Spectroscopy of Proteins, Springer, Berlin, 1986.
- Draganski A. and Ludescher R. D., 2010. Phosphorescence from Single Tryptophan in Amorphous Solid Human Serum Albumin Exhibits Solvent-Protein Dynamics Slaving. *Biophys. J.* 98 (3): 226a.
- Dranca I., Bhattacharya S., Vyazovkin S. and Suryanarayanan R., 2009. Implications of global and local mobility in amorphous sucrose and trehalose as determined by differential scanning calorimetry. *Pharma. Res.* 26 (5): 1064-1072.
- Ekdawi-Sever N. C., Conrad P. B., de Pablo J. J., 2001. Molecular Simulation of Sucrose Solutions near the Glass Transition Temperature. *J. Phys. Chem. A*, 105(4): 734-742.
- Fennema, O. 1976. Food Chemistry, Part I (Principles of Food Science Series). O. Fennema, editor. Marcel Dekker, New York.
- Fischer C. J., Gafni A., Steel D. G., Schauerte J. A. 2001. The triplet-state lifetime of indole in aqueous and viscous environment: significance to the interpretation of room temperature phosphorescence in proteins. *J. Am. Chem. Soc.* 124: 10359-10366.
- Goff H. D., Caldwell K. B., Stanley D. W., 1993. The Influence of Polysaccharides on the Glass Transition in Frozen Sucrose Solutions and Ice Cream. *J. Dairy Sci.* 76: 1268-1277.
- Gonnelli M. G. and Strambini G. B., 1995. Phosphorescence lifetime of tryptophan in proteins. *Biochem.* 34: 13847-13857.
- Gonnelli M. G., Strambini G. B., 2005. Intramolecular quenching of tryptophan phosphorescence in short peptides and protein. *Photochem. Photobiol.* 81: 614-622.
- Green j. and Angell C. A., 1989. Phase relations and vitrification in saccharide-water Solutions and the Trehalose Anomaly. *J. Phys. Chem.* 93: 2880-2882.
- Hott J. L. and Borkman R. F. 1989. The non-fluorescence of 4-fluorotryptophan. *Biochem. J.* 264: 297-299.
- Hancock B. C., Shamblin S. L., and Zografi G., 1995. Molecular mobility of amorphous pharmaceutical solids below their glass transition temperatures. *Am. Assoc. Pharm. Sci.* 12(6): 799-806.

- Hancock B. C. and Zografi G. 1997. Characteristics and significance of the amorphous state in pharmaceutical systems. *J. Pharm. Sci.* 86: 1-12.
- Hancock B. C. and Dalton, C. R. 1999. The effect of temperature on water vapor sorption by some amorphous pharmaceutical sugars. *Pharm. Dev. Technol.* 4 (1): 125-131.
- Hünig I. and Kleineremanns K., 2004. Conformers of the peptides glycine-tryptophan, tryptophan-glycine and tryptophan-glycineglycine as revealed by double resonance laser spectroscopy. *Phys. Chem. Chem. Phys.* 6: 2650-2658.
- Ilich P., 1995. 7-Azaindole: the low-temperature near-UV/vis spectra and electronic structure. *J. Mol. Struct.* 354 (1):37-47.
- Ingham K. C., El-Bayoumi M. A. 1974. Photoinduced double proton transfer in a model hydrogen bonded base pair and deuterium substitution effects of temperature. *J. Am. Chem. Soc.* 96(6): 1674-1682.
- Jouppila K. and Roos Y. H., 1994. Glass transitions and crystallization in milk powder. *J. Dairy. Sci.* 77(10): 2907-2915.
- Limbach H. J. and Ubbink J., 2008. Structure and dynamics of maltooligomer–water solutions and glasses. *Soft Matter* 4: 1887-1898.
- Liu Y., Bhandari B., Zhou W., 2006. Glass transition and enthalpy relaxation of amorphous food saccharides: A review. *J. Agric. Food Chem.* 54: 5701-5717.
- Ludescher R. D., Shah N. K., McCaul C. P., Simon K. V., 2001. Beyond T_g: optical luminescence measurements of molecular mobility in amorphous solid foods. *Food Hydrocolloids* 15: 331-339.
- Matsui K., Matsuzuka T., Fujita H. 1989. Fluorescence spectra of 7-azaindole in the sol-gel-xerogel stages of silica. *J. Phys. Chem.* 93: 4991-4994.
- McCaul C. P. and Ludescher R. D., 1999. Room temperature phosphorescence from tryptophan and halogenated tryptophan analogs in amorphous sucrose. *Photochem. photobiol.* 70 (2): 166-171.
- Meloun B., Moravek L. Kostka V., 1975. Complete amino acid sequench of human serum albumin. *FEBS Lett.* 58 (1): 134-137.
- Miller D. P., Depablo J.J., Corti H., 1997. Thermophysical properties of Trehalose and its concentrated aqueous aolutions. *Am. Assoc. Pharm. Sci.* 14(5): 578-590.
- Neidigh J. W., Fesinmeyer R. M., Andersen N. H., 2002. Designing a 20-residue protein. *Nat. Struc. Biol.* 9 (6): 425-430.
- Noel T. R., Parker R., Ring, S. G., 2000. Effect of molecular structure and water content on the dielectric relaxation behaviour of amorphous low molecular weight carbohydrates above and below their glass transition. *Carbohydr. Res.* 329: 839-845.
- Phillips J. C., 2006. Ideally glassy hydrogen-bonded networks. *Phys. Rev. B: Condensed Matter.* 73: 10194-10192.
- Pouton C. W., 2006. Formulation of poorly water-soluble drugs for oral administration: physicochemical and physiological issues and the lipid formulation classification system. *Eur. J. Pham. Sci.* 29: 278-287.

- Pravinata L. C., You Y. and Ludescher R. D., 2005. Erythrosin B phosphorescence monitors molecular mobility and dynamic site heterogeneity in amorphous sucrose. *Biophys. J.* 88 (5): 3551-3561.
- Qiu L., Pabit S. A., Roirberg A. E., Hagen S. J., 2002. Smaller and Faster: The 20-Residue Trp-Cage Protein Folds in 4 μ s. *J. Am. Chem. Soc.* 124:12952-12953.
- Richert, R. 2000. Triplet state solvation dynamics: basics and applications. *J.Chem.Phys* 113: 8804-8429.
- Rossi S., Moreno S., Chirife J., 1997. Stabilization of the restriction enzyme *EcoRI* dried with trehalose and other selected glass-forming solutes. *Biotech. Prog.* 13(5): 609-616.
- Sengupta B., Guharay J., Chakraborty A., Sengupta P. K., 2002. Low temperature luminescence behaviours of 7-azatryptophan, 5-hydroxytryptophan and their chromophoric moieties. *Spectrochim. Acta, Part A* 58: 2005-2012.
- Serrano-Andr  s L. and Borin A. C., 2000. Theoretical study of the emission spectra of indole and its analogs: indene, benzimidazole, and 7-azaindole. *Chem. Phys.* 262: 267-283
- Shah N. K., Ludescher R. D. 1995. Phosphorescence probes of the glassy state in amorphous sucrose. *Biotech. Prog.* 11:540-544.
- Shamblin S. L., Tang X., Chang L., Hancock B. C., Pikal M. J., 1999. Characterization of the Time Scales of Molecular Motion in Pharmaceutically Important Glasses. *J. Phys. Chem. B* 103 (20): 4113-4121.
- Shemesh D., H  ttig C., Domcke W., 2009. Photophysics of the Trp-Gly dipeptide: Role of electron and proton transfer processes for efficient excited-state deactivation. *Chem. Phys. Lett.* 482: 38-43.
- Shemesh D., Sobolewski A. L., Domcke W., 2008. Efficient excited-state deactivation of the Gly-Phe-Ala tripeptide via an electron-driven proton-transfer process. *J. Am. Chem. Soc.* 131: 1374-1375.
- Shirke S., You Y., Ludescher R. D., 2006. Molecular mobility and dynamic site heterogeneity in amorphous lactose and lactitol from erythrosin B phosphorescence. *Biophys. Chem.* 123: 122-133.
- Steiner R.F. and Weinryb I. 1968. The luminescence of tryptophan and phenylalanine derivatives. *Biochem.* 7 (7): 2488-2495.
- Streicher W. W. and Makhatadze G. I. 2007. Unfolding thermodynamics of Trp-Cage, a 20 residue miniprotein, studied by differential scanning calorimetry and circular dichroism spectroscopy. *Biochem.* 46: 2876-2880.
- Sun W. Q. and Leopold A. C., 1997. Cytoplasmic vitrification and survival of anhydrobiotic organisms. *Comp. Biochem. Physiol.* 117A: 327-333.
- Sun W. Q. and Davidson P., 1998. Protein inactivation in amorphous sucrose and trehalose matrixes: effect of phase separation and crystallization. *Biochem. Biophys. Acta.* 1425: 235-244.
- Taylor C. A., El-Bayoumi M. A., Kasha M., 1969. Excited-state two-proton tautomerism in hydrogen-bonded N-heterocyclic base pairs. *PNAS* 63(2): 253-260.

- Townrow S., Kilburn D., Alam A., and Ubbink j., 2007. Molecular packing in amorphous carbohydrate matrixes. *J. Phys. Chem. B* 111(44): 12643-12648.
- Valdés H., Reha D., Hobza P., 2006. Structure of isolated tryptophyl-glycine dipeptide and tryptophyl-glycyl-glycine tripeptide: ab initio SCC-DFTB-D molecular dynamics simulations and high-level correlated ab initio quantum chemical calculations. *J. Phys. Chem. B* 110: 6385-6396.
- Wang W. 1999. Instability, stabilization and formulation of liquid protein pharmaceuticals. *Int. J. Pharm.* 185: 129-188.
- Yoshioka S., Aso Y., 2007. Correlations between molecular mobility and chemical stability during storage of amorphous pharmaceuticals. *J. Pharm. Sci.* 96(5): 960-981.
- You Y., Ludescher R. D., 2008. The effect of sodium chloride on molecular mobility in amorphous sucrose detected by phosphorescence from the triplet probe erythrosin B. *Carbohydr. Res.* 342 (2): 350-363
- You Y. and Ludescher R. D., 2010. The effect of molecular size on molecular mobility in amorphous oligosaccharides. *Food Biophys.* 5: 82–93.
- Zallen R. 1983. The physics of amorphous solids. John Wiley & Sons. New York
- Zhou D., Zhang G., Law D., Grant D. J.W., Schmitt E. A., 2002. Physical stability of amorphous pharmaceuticals: importance of configurational thermodynamic quantities and molecular mobility. *J. Pharm. Sci.* 91(8): 1863-1872.
- Zhou R., 2003. Trp-cage: Folding free energy landscape in explicit water. *PNAS.* 100(23): 13280-13285.